

NACA TN 2997

NATIONAL ADVISORY COMMITTEE FOR AERONAUTICS

TECHNICAL NOTE 2997

APPLICATION OF SEVERAL METHODS FOR DETERMINING
TRANSFER FUNCTIONS AND FREQUENCY RESPONSE
OF AIRCRAFT FROM FLIGHT DATA

By John M. Eggleston and Charles W. Mathews

Langley Aeronautical Laboratory
Langley Field, Va.



Washington
September 1953
FOR REFERENCE

NOT TO BE TAKEN FROM THIS ROOM

LANGLEY AERONAUTICAL LABORATORY
Langley Field, Va.

NATIONAL ADVISORY COMMITTEE FOR AERONAUTICS

TECHNICAL NOTE 2997

APPLICATION OF SEVERAL METHODS FOR DETERMINING
TRANSFER FUNCTIONS AND FREQUENCY RESPONSE
OF AIRCRAFT FROM FLIGHT DATA

By John M. Eggleston and Charles W. Mathews

SUMMARY

In the process of analyzing the longitudinal frequency-response characteristics of aircraft, information on some of the methods of analysis has been obtained by the Langley Laboratory of the National Advisory Committee for Aeronautics. In the investigation of these methods, the practical applications and limitations were stressed.

In general, the methods considered may be classed as: (1) analysis of sinusoidal response, (2) analysis of transient response as to harmonic content through determination of the Fourier integral by manual or machine methods, and (3) analysis of the transient through the use of least-squares solutions of the coefficients of an assumed equation for either the transient time response or frequency response (sometimes referred to as curve-fitting methods).

The investigation has led to the following observations: The curve-fitting methods (Donegan-Pearson and exponential-approximation methods) appear to be less critical to inputs having regions of low harmonic content than Fourier methods and present the frequency response as analytical expressions (transfer functions). Fourier methods indicate characteristics of frequency response that may be missed in curve-fitting methods because of the limitations on the assumed form of the equations used in the curve-fitting methods. For manual calculations, the Donegan-Pearson method appears to be best suited for highly damped systems in response to arbitrary control inputs, the exponential-approximation method appears to be best suited for lightly damped systems in response to step or short-pulse control inputs, and the Fourier method offers comparable results but requires lengthy calculations. Special machines for performing the Fourier analysis, such as the Coradi harmonic analyzer and the Fourier synthesizer, reduce the time required for the solution but do not offer particular improvement in accuracy over the usual manual methods. The use of punch-card calculating machines for the evaluation of the Fourier integrals appears to offer possibilities of more accurate results with a large reduction in time over the usual manual methods.

INTRODUCTION

In recent years, a large number of methods have been advanced for the purpose of obtaining frequency-response data, transfer functions, and stability coefficients from flight tests by using control inputs of arbitrary shape. As pointed out in reference 1, the data obtained from the application of these methods are of great value to aircraft and autopilot designers as well as to designers of other electronic airborne equipment for the combination of their individual products into a stable working unit.

A résumé of methods and progress to date with reference to dynamic flight testing is presented by Milliken in reference 2. Although all these methods appear to have advantages and limitations, some methods have gained popularity with various groups whereas other methods remain comparatively unused. A number of methods have been examined and used by the Flight Research Division of the Langley Aeronautical Laboratory in an effort to determine which methods to adopt in establishing the transfer functions of the various aircraft undergoing dynamic flight tests. This program has offered a certain amount of practical experience in the use and limitations of the methods, and it is believed that this experience may be of value to others engaged in obtaining the frequency responses of aircraft. No attempt has been made to examine all the known methods of analyzing dynamic responses and omission of any method is not intended to imply lack of merit.

A brief review of the methods examined is offered in this paper, together with references to their derivations and examples of their application. Three types of aircraft, a fighter, a transport, and a free-fall model, were used for these examples. The examples are concerned with the short-period longitudinal mode of the airplane, which is usually a well-damped mode defined by a fairly simple transfer function. Thus, the comparisons of methods presented herein are made solely on the basis of results obtained from analysis of this longitudinal mode. It is recognized that complicated oscillating systems may be analyzed and greater accuracies obtained by all the methods reported at the expense of a more extensive analysis. The comparison of methods presented herein, however, may be altered when applied to more complicated systems.

The methods are discussed with regard to the time required, the means for facilitating their use, and the limitations on their application. Some opinions presented are not directly substantiated by quantitative results but are based on experience in the use of the methods. The results obtained are compared to give some indication of the relative accuracy of the methods, exclusive of any inaccuracy in the measurements.

SYMBOLS

A,B,C,E,F, G,H,L,M,N }	coefficients of longitudinal transfer functions of an airplane (composed of stability parameters)
A	amplitude
a,b,c,d	coefficients of cubic approximation to transient
a	damping exponent in e^{at}
b	damping coefficient, $-2a$
C	arbitrary coefficient
D	differential operator, d/dt
e	natural logarithmic base, 2.71828
h_p	pressure altitude, ft
J_1, J_2	coefficients of equation relating airplane longitudinal response to step-control motion
$j = \sqrt{-1}$	
K_1, K_2	real and imaginary terms of Fourier integral, respectively
k	stiffness coefficient, $a^2 + \omega^2$
M	Mach number
m	numerical integer
n	numerical integer or normal acceleration, g units
P	period, sec
p	Laplace transform variable
Q	quantity as a function of frequency
q	quantity as a function of time
T	time variable of integration, sec

$T_{1/2}$	time to damp to one-half amplitude, sec
$T_{1/20}$	time to damp to one-twentieth amplitude, sec
t	time, sec
t_p	time required for oscillation to reach initial peak from time of step-control input, sec
t_r	time interval over which curve analyzed
x	abscissa of response curves
y	ordinate of response curves
α	angle of attack, deg
γ	flight-path angle, deg
δ	control deflection, deg
ζ	damping ratio, $\frac{\text{Damping coefficient}}{\text{Critical damping coefficient}}$
θ	pitch angle, deg
τ	time lag, sec
ϕ	phase angle, deg
ψ_1, ψ_2	displacement coefficients of Coradi harmonic analyzer
ω	frequency, radians/sec
ω_n	undamped natural frequency, radians/sec
ω_o	forcing frequency, radians/sec
Subscripts:	
e	elevator
I	input
O	output

- o magnitude at $t = 0$
- ss magnitude at steady state
- ∞ magnitude at infinity
- e error
- 0,1,2,3,...n numerical integers

The absolute value of any term is denoted by $| \quad |$.

BASIC CONCEPTS

It is assumed herein that the reader is familiar with the concepts and application of the Laplace transform to linear systems. A presentation of this method may be found in reference 3.

The frequency response of a dynamic system defines its steady-state response under the influence of an input applied in the form of a sinusoidal oscillation of constant amplitude and period. An analytical expression which defines the frequency response throughout the frequency range is, when defined in terms of the Laplace transform variable p , the transfer function of the system. The transfer function not only expresses the frequency response but it may be said that, for linear systems, any arbitrary input function operated on by the transfer function determines the variation in the output function. Conversely, if the input and output are known, it should be possible to determine an analytical expression which relates the two, that is, the transfer function. The present paper is concerned with several methods of obtaining the transfer functions of aircraft from measured inputs and responses. The methods presented herein, in general, may be divided into two classes: methods that first determine the frequency response of the system and methods that determine the transfer function without the determination of the frequency response.

The NACA sign convention, as shown in figure 1, assumes elevator trailing edge down as positive. Therefore, a positive elevator deflection will, in general, produce negative static responses. In order to conform with the usual practice of plotting frequency-response data, phase angles have been shifted 180° (that is, zero phase angle at zero frequency).

DESCRIPTION AND DISCUSSION OF METHODS

Sinusoidal-Response Method

Of the several possible ways to obtain the frequency response of a system, an obvious way is to oscillate sinusoidally a control surface at a constant amplitude and frequency until a steady-state response of the aircraft has been obtained and measure the amplitude and phase relationship between input and output sine waves. The process may then be repeated throughout the frequency range of interest. The theoretical application of this method to the determination of the coefficients of the transfer function is given by Greenberg in reference 4, and a graphical method of determining transfer functions from frequency-response data is given in reference 5.

The sinusoidal-response method requires the least computation time and the most flight time of the methods reported herein. In an effort to reduce the large amount of flight testing required, a number of simplifications from the usual technique have been attempted. One procedure that was investigated involved obtaining sinusoidal-response data by continuously recording the controlled input and the response of the airplane while slowly changing the frequency of the input to cover the range of frequencies desired. Appendix A presents an estimation of the errors encountered at several values of rate of change of forcing frequency when such a frequency-modulated input is applied to a dynamic system defined by a second-order lag. From this analysis and also from flight results, it appears that, for systems having near critical damping, satisfactory results may be obtained. In addition, it appears that a human pilot may generate an adequately near sinusoidal input without the aid of special equipment, particularly if he has a fairly precise indication of the amplitude of his stick motion. A typical record obtained by using these techniques is presented in figure 2. The deviation from a pure sinusoidal input is obvious although the filtering supplied by the airframe results in a nearly sinusoidal response. Jones and Sternfield in reference 6 outline a method for determining the amplitude of an equivalent sine wave when the actual periodic wave has an irregular form. In general, however, it has been possible to obtain results consistent with the accuracy of the measurements by fairing the peaks of the oscillations in the input and output and obtaining the double amplitude of these quantities from the fairing by averaging over a number of successive half-cycles. The mean value about which the oscillations occur is established from the fairing of the peak amplitudes, and the time lag of the output behind the input is determined by averaging the lag read along this mean value over a number of successive half-cycles. The period of the oscillations is similarly obtained by averaging. The method of measurement of these quantities is illustrated in figure 2.

The importance of averaging over successive half-cycles, when establishing the time lag, is shown in figure 2 where, in some cases, the velocity of the input is considerably different in one direction than in the other with the result that the time lag read at one point will differ considerably from that read one-half period later. The average, however, appears, in most cases, to represent adequately the actual time lag.

The frequency-response parameters may be determined from the averaged values through use of the following relations:

$$\text{Frequency} = \frac{2\pi}{\text{Period}} \quad (1)$$

$$\text{Amplitude ratio} = \frac{\text{Amplitude of output}}{\text{Amplitude of input}} \quad (2)$$

$$\text{Phase angle} = 360 \frac{\text{Lag}}{\text{Period}} \quad (3)$$

Flight records for a fighter airplane were obtained with the pilot manually applying an approximate sine wave of varying frequency to the elevator. A sample of the flight data is presented in figure 2 and some pertinent geometric characteristics of the airplane and the flight condition under which the data were obtained are listed in table I. Data points obtained by the foregoing analysis are presented in figure 3 together with a suggested fairing. The scatter is considered typical for this technique (pilot-induced input). These data points represent portions of two flights of the fighter airplane and a recording time of about 250 seconds. A typical example of the time required to reduce the flight data to a frequency-response curve by this method is shown in table II. Typical times are also presented in the table for other methods to be discussed subsequently.

Fourier Analysis of Transient Response

Another well-known method of determining the frequency response is to determine the coefficients of the Fourier transform of the input and output functions over a frequency range by analyzing the response (as a

function of time) of the aircraft to an arbitrary input. The process is indicated by the expression

$$\frac{q_O}{q_I}(j\omega) = \frac{\int_0^{\infty} q_O(t) e^{-j\omega t} dt}{\int_0^{\infty} q_I(t) e^{-j\omega t} dt} \quad (4)$$

which represents the ratio of the Fourier integral of the output to the Fourier integral of the input. The derivation and several applications of this method are reported in references 4 and 7.

This method, as well as the sinusoidal method previously described, gives data points in amplitude ratio and phase angle at a number of discrete frequencies through which a fairing can be made. Transfer functions may be obtained from the frequency-response curves by the same methods as were mentioned for the sinusoidal response.

Integration of the Fourier integral offers a choice of methods which may be divided into two general categories: (1) methods which divide the transient into finite intervals, approximate the curves within each interval with an analytical expression, perform the indicated integration analytically, and sum the real and imaginary parts of these integrals; and (2) methods which express $e^{-j\omega t}$ in trigonometric form, multiply these sine and cosine functions by the value of $q(t)$ at corresponding times, and integrate the product curves to determine the real and imaginary terms of the Fourier integral.

Solution of the Fourier integral by either approach involves the judicious choice of time intervals. For the analytical representation method, a choice in the form of the analytical expression must also be made. As the chosen expression becomes more complex, the accuracy of the determination of the frequency response generally increases but, as the work involved likewise increases, a compromise usually is necessary.

The following are several methods which have been studied and illustrate the various approaches to the Fourier transformation.

Manual Method: Analytical integration within discrete intervals of cubic representations of a transient.- A method of representing a transient for solution of the Fourier integral, as developed by Ordway B. Gates, Jr., of the Langley Laboratory, involves the division of the transient into discrete time intervals chosen to facilitate accurate

approximation of each portion of the transient by cubic (or lower-order) polynomials. The Fourier integral will then be

$$\begin{aligned}
 Q(\omega) &= \int_0^{\infty} q(t)e^{-j\omega t} dt \\
 &= \int_0^{t_1} q_0(t)e^{-j\omega t} dt + \int_{t_1}^{t_2} q_1(t)e^{-j\omega t} dt + \dots + \\
 &\quad \int_{t_n}^{t_{n+1}} q_n(t)e^{-j\omega t} dt + \dots + \int_{t_{ss}}^{\infty} q_{ss}(t)e^{-j\omega t} dt \quad (5)
 \end{aligned}$$

where

$$q_n(t) = a_n t^3 + b_n t^2 + c_n t + d_n$$

The values of the coefficients a_n , b_n , c_n , and d_n for any given n may be determined from the characteristics of the transient within the interval t_n to t_{n+1} . For the general case, the interval is subdivided into thirds and values of the transient $q(t)$ at these dividing points afford four cubic equations having four unknowns (a_n , b_n , c_n , and d_n). The advantage of using equal divisions within the interval t_n to t_{n+1} is the ease of the solution of the four equations by means of "successive subtraction." (See illustrated example in appendix B.) If, however, the slope of the transient is zero ($\frac{dq}{dt} = 0$) within the interval, this condition should be used as well as the value of the transient $q(t)$ at this point. The coefficients thus determined give an equation that may be used to check the fit of the transient by the expression before further work is initiated.

This approach to the evaluation of the Fourier integral may be expressed analytically as follows:

$$Q(\omega) = \sum_{n=0}^{n=ss} Q_n(\omega) = K_1(\omega) - jK_2(\omega) \quad (6)$$

where

$$Q_n(\omega) = \int_{t_n}^{t_{n+1}} (a_n t^3 + b_n t^2 + c_n t + d_n) e^{-j\omega t} dt$$

and

$$a_n \int_{t_n}^{t_{n+1}} t^3 e^{-j\omega t} dt = -\frac{a_n}{\omega^4} (6 + 6j\omega t - 3t^2\omega^2 - jt^3\omega^3) e^{-j\omega t} \Big|_{t_n}^{t_{n+1}}$$

$$b_n \int_{t_n}^{t_{n+1}} t^2 e^{-j\omega t} dt = \frac{b_n}{j\omega^3} (2 + 2j\omega t - t^2\omega^2) e^{-j\omega t} \Big|_{t_n}^{t_{n+1}}$$

$$c_n \int_{t_n}^{t_{n+1}} t e^{-j\omega t} dt = \frac{c_n}{\omega^2} (1 + j\omega t) e^{-j\omega t} \Big|_{t_n}^{t_{n+1}}$$

$$d_n \int_{t_n}^{t_{n+1}} e^{-j\omega t} dt = -\frac{d_n}{j\omega} e^{-j\omega t} \Big|_{t_n}^{t_{n+1}}$$

The substitution of discrete values of frequency ω gives the real and imaginary terms of the Fourier transform of the time transient $q(t)$, and the relationships of amplitude and phase are given as.

$$\left. \begin{aligned} A &= \sqrt{K_1^2 + K_2^2} \\ \phi &= \tan^{-1} \frac{-K_2}{K_1} \end{aligned} \right\} \quad (7)$$

As an illustration of this method, a numerical example is presented in appendix B. A method of this type is not very adaptable to machine

methods because some discretion is required in the subdivision of the transient, and the time intervals are not necessarily equal. A small amount of trial and error may be required in the choice of these time intervals, particularly in the vicinity of points of inflection. The cubic representation has the merit of being the lowest-order polynomial to contain a point of inflection. This approach to the solution of the Fourier integral has the advantage of providing an analytical representation that may be directly compared with the transient and of providing an exact analytical integration. On the basis of comparable accuracy, this approach is in many instances shorter than the classical numerical integration method that follows.

Manual Method: Numerical integration of product curves of $q(t)\sin \omega t$ and $q(t)\cos \omega t$. - The usual manual method, which also is the basis of some of the machine methods, requires a large amount of graphical or numerical integration because no attempt is made to obtain a continuous analytic expression for the transient until it has reached a steady state. If the input is restricted to a simple analytical expression (for example, a step input will have a constant value from zero time to infinity), the graphical or numerical integration of the input is eliminated and the time required for the solution of equation (4) is roughly reduced by one-half. For the purpose of graphical or numerical integration, equation (4) may be reduced to an expression involving real integrals of the form

$$\int_0^{\infty} q(t)e^{-j\omega t} dt = \int_0^{\infty} q(t)\cos \omega t dt - j \int_0^{\infty} q(t)\sin \omega t dt$$

$$= K_1(\omega) - jK_2(\omega) \tag{8}$$

where the frequency-response relationships are given by equation (7).

The numerical and graphical method for the solution of the Fourier integral and an example of its use is given in reference 4 by Greenberg and a more complete discussion is given by Schetzer in reference 8.

A rule of thumb for choosing the proper time interval in analyzing flight data has been suggested by experience gained in the use of this technique. The rule is restricted to the methods of integration adaptable to the manual methods, for example, Simpson's three-point rule. In general, a chosen time interval Δt will give reasonable results up to a frequency of $\frac{\pi}{5 \Delta t}$ so that a time interval of 0.10 second may

be expected to produce good results up to a frequency of about 6 radians per second. The proper choice of time intervals is obviously dependent on the character of the input and output; however, the foregoing rule has been found usually conservative except in cases of extremely erratic variations in the input and output. The highest frequency at which reasonable results might be expected will also depend upon the choice of forms of integration, a superior integrating method affording use of greater time intervals for comparable results.

When Simpson's three-point rule for numerical integration or a planimeter are used for this method, the time required may be estimated by another rule gained from experience. For a typical case where the short-period longitudinal response to a step or pulse input is analyzed, the time required to obtain the amplitude and phase angle of the output (one) function at 8 frequencies by using 24 data points has been found to be about 6 man-hours for an experienced user. Tabulated values of $\sin \omega t$ and $\cos \omega t$ were used and the time required to make these tabulations was not included in the estimate.

Punch-card method (IBM).— Certain International Business Machines (described subsequently and referred to as IBM machines) offer a time-saving solution to the process outlined in the previous section with usually more accurate results over a greater frequency range since use of more complicated and accurate methods of numerical integration are feasible. Weddle's seven-point rule (ref. 9, p. 125) as derived from the Newton-Cotes quadrature formula has been employed and is an example of such a method.

By using essentially the same procedure as the manual method which integrates the product curves $q(t)\sin \omega t$ and $q(t)\cos \omega t$, a set of "master" cards are punched which define the values of the cosine and sine functions for the values of ωt selected and also define the numerical integration process used. Since values of ωt determine the values of the trigonometric functions punched on the cards, the frequency range to be evaluated may be varied by changing the time interval in inverse proportion. Cards are likewise punched for the time functions of input and output (and these must obviously be punched for each separate analyzed record).

The calculations involved in the Fourier analysis method as performed on the IBM machines that are available at the Langley Laboratory are as follows:

- (1) Time response data are perforated onto IBM cards by using a card punch.
- (2) Correct transcription of data onto cards is checked by a varifier.

(3) Original deck of cards representing time-response data is reproduced, one deck for each frequency to be analyzed, by using a reproducer.

(4) Integrating factors and trigonometric functions are transferred from the "master" deck to each deck obtained from step (3) by using the reproducer.

(5) Product functions ($q(t)\sin \omega t$ and $q(t)\cos \omega t$) are obtained by an electronic calculator.

(6) End corrections and integration corrections are applied by using a sorter and the electronic calculator.

(7) Fourier summation of terms obtained for each frequency are made by using a tabulator (alphabetical accounting machine).

(8) Summary cards of amplitude and phase relationships are obtained on the electronic calculator.

(9) Final frequency data of input and output functions are typed out by the tabulator.

Some aspects of this process as applied to lateral responses having steady-state oscillatory responses are described in more detail in reference 10.

The time required for this IBM equipment to perform the operations indicated has been found to be 5 machine-hours for the determination of data at 12 frequencies for one function by using one set of machines and 241 data points (12-second records using 0.05-second intervals). This time was averaged over several performances and included all checks and correction of mistakes.

Method using the electromechanical Fourier synthesizer.- The electromechanical Fourier synthesizer, originally built and used by the Massachusetts Institute of Technology to produce transient-response curves from frequency-response data, was designed to perform the following operation (see ref. 11):

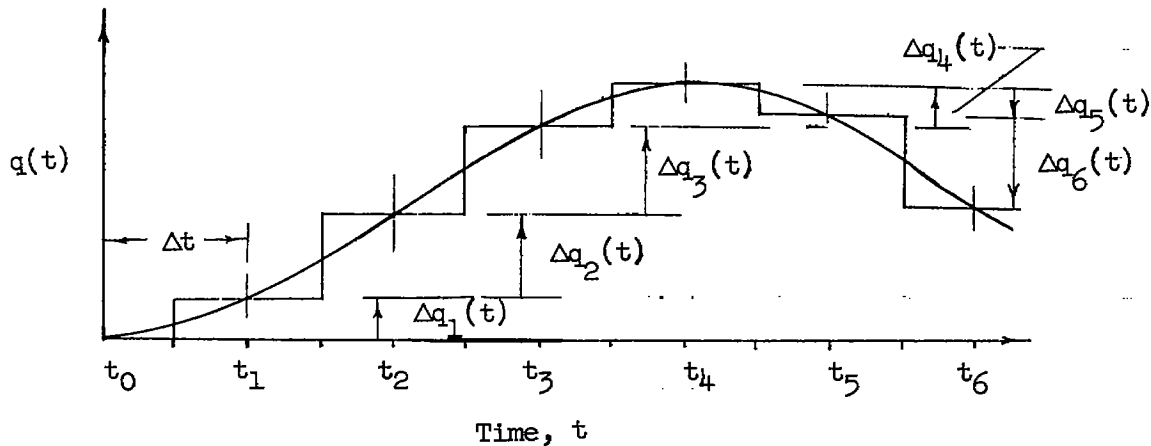
$$\sum_{n=1,2,3,\dots} q_n e^{-j(n\beta + \phi_n)} = \sum_{n=1,2,3,\dots} q_n \cos(n\beta + \phi_n) - j \sum_{n=1,2,3,\dots} q_n \sin(n\beta + \phi_n) \quad (9)$$

where

- q_n amplitude of nth harmonic
- ϕ_n phase angle of nth harmonic
- β angular displacement of fundamental

The application of the Fourier synthesizer to the evaluation of the Fourier integral may be seen from the following derivation.

The general form of analysis assumes that any arbitrary curve of input or output may be represented by a series of step functions with a constant finite time lag between the steps:



The step approximation is the same as that used in the analytical method of obtaining the frequency response from a time response to a step input as presented in reference 12 and also the same as the extension of this analytical method to an arbitrary input as presented in reference 13. Thus, the Fourier integral of an arbitrary function in time $q(t)$ may be approximated in the form

$$Q(\omega) = \int_{t_1 - \frac{\Delta t}{2}}^{\infty} \Delta q_1(t) e^{-j\omega t} dt + \int_{t_2 - \frac{\Delta t}{2}}^{\infty} \Delta q_2(t) e^{-j\omega t} dt + \dots + \int_{t_n - \frac{\Delta t}{2}}^{\infty} \Delta q_n(t) e^{-j\omega t} dt \quad (10)$$

Therefore,

$$Q(\omega) = \frac{1}{j\omega} \sum_{n=1,2,3,\dots} \Delta q_n(t) e^{-j\left(n\omega \Delta t - \omega \frac{\Delta t}{2}\right)} \quad (11)$$

In trigonometric form

$$Q(\omega) = -\frac{1}{\omega} \sum_{n=1,2,3,\dots} \Delta q_n(t) \sin\left(n\omega \Delta t - \omega \frac{\Delta t}{2}\right) - \frac{j}{\omega} \sum_{n=1,2,3,\dots} \Delta q_n(t) \cos\left(n\omega \Delta t - \omega \frac{\Delta t}{2}\right) \quad (11a)$$

This relationship, as can be seen by comparison of equation (11a) with equation (9), may be handled by the Fourier synthesizer.

The number of points that may be used conveniently to represent the time-response curve is determined by the number of resolvers available in the machine to simulate the convolution process. The machine investigated, employing 24 resolvers, required 4 to 8 hours to obtain the frequency response of a system from any arbitrary input and output that may be represented by 24 equally spaced steps. The frequency data are presented by the machine as curves of the Fourier transforms of the real and imaginary coefficients. From these curves, values at any number of frequencies may be chosen for the determination of phase angle and amplitude.

In view of the fact that the Fourier synthesizer utilizes 24 equally spaced steps, it is limited to transients that may be adequately approximated thereby. Although the frequency range plotted by the synthesizer is from 0 to $\pi/\Delta t$ radians per second, the results do not appear to be accurate to any higher frequency range than is quoted for the manual method which uses Simpson's rule ($\omega = \frac{\pi}{5 \Delta t}$).

Coradi harmonic analyzer.- The Coradi harmonic analyzer (ref. 14) is a semimanually operated tracing machine which by the use of several rolling spheres may be used to evaluate the Fourier integral of a function. The model investigated (Dent-Draper Model, Rolling Sphere Type, Mico Instrument Company, Cambridge, Mass.) employed five spheres which, through use of various gears, may measure the harmonic content of a curve within a range of 1 to 50 harmonics. Details of the operation of an earlier model of the Coradi harmonic analyzer are presented in reference 15.

Through the use of the Coradi harmonic analyzer, the time transient is traced from the point of initiation (initial conditions zero) to the point of steady-state response and the following integrals are evaluated:

$$\psi_1 = -C \int_{y_0}^{y_{ss}} \cos \omega t \, d[y(t)] \quad (12a)$$

$$\psi_2 = C \int_{y_0}^{y_{ss}} \sin \omega t \, d[y(t)] \quad (12b)$$

These integrals are proportional to the real and imaginary part of the Fourier integral of the curve being analyzed

$$Q(\omega) = \int_0^{\infty} q(t) e^{-j\omega t} dt$$

The proportionality may be seen by integrating the Fourier integral by parts to change variables so that

$$Q(\omega) = - \frac{q(t)}{j\omega} e^{-j\omega t} \Big|_0^{\infty} + \frac{1}{j\omega} \int_0^{q(\infty)} e^{-j\omega t} d[q(t)] \quad (13)$$

where for all practical purposes the first term is zero. In the use of the Coradi harmonic analyzer, the term $q(t)$ is plotted along the y-axis; therefore, equation (13) may be written as follows:

$$\begin{aligned}
 Q(\omega) &= \frac{1}{j\omega} \int_0^{y_\infty} e^{-j\omega t} d[y(t)] \\
 &= \frac{1}{j\omega} \int_0^{y_{ss}} e^{-j\omega t} dy + \frac{1}{j\omega} \int_{y_{ss}}^{y_\infty} e^{-j\omega t} d[y(t)] \quad (14)
 \end{aligned}$$

where the second term is zero since $y_{ss} = y_\infty$. In trigonometric form, equation (14) becomes

$$Q(\omega) = -\frac{1}{\omega} \int_0^{y_{ss}} \sin \omega t d[y(t)] + \frac{1}{j\omega} \int_0^{y_{ss}} \cos \omega t d[y(t)] \quad (15)$$

so that substitution of equations (12) into equation (15) gives

$$Q(\omega) = \frac{-\psi_2}{\omega C} + j \frac{\psi_1}{\omega C} \quad (16)$$

where $\omega = \frac{2\pi n}{t_r}$ and t_r is defined as the time interval over which the curve was analyzed. The constant $1/C$ is the scale factor between the function being analyzed and the displacement of the dials of the analyzer. In general, because only the ratio of output to input is desired, the individual scale factors need not be computed provided both quantities are plotted to the same scale.

This analyzer appears to produce the Fourier coefficients within an accuracy dependent upon the kinematic accuracy of the machine (which is primarily affected by slipping of the rollers but also to some extent by wear) and the ability of the operator and machine to follow exactly the trace being analyzed. The operator is required to follow the curve in the direction of the ordinate $q(t)$ while the machine, operated by a microswitch, automatically traverses along the abscissa t . Accurate tracing becomes difficult when steep slopes (large values of dq/dt) are experienced, and a certain amount of roller slipping and human error

should be expected. This inaccuracy is alleviated somewhat by averaging the values obtained from three or more repeated tracings. Experience with the machine has indicated that the accuracies obtained are about the same as those obtained by the manual methods.

The time required to obtain the Fourier coefficients of one function $q(t)$ for 15 harmonics has been found to be about 4 hours for an experienced operator. This estimate includes the time to aline correctly the axes of the curve with the machine, to connect the correct set of gears for each 5 harmonics, and to trace the curve three times for each set of 5 harmonics.

A consideration in the use of this machine is its ability to produce the Fourier coefficients in a comparatively short time, particularly with erratic functions that would require very small time intervals to represent accurately the function for use by other methods. A point worth noting is that, for erratic functions, the average of several tracings should produce a more reliable result. In the use of the Coradi harmonic analyzer, the limitation that the function must reach steady state still applies.

Curve-Fitting Methods

In the methods herein called curve-fitting methods, the form of the transfer function is directly or indirectly assumed and the coefficients of the transfer function are determined by least-squares methods or a combination of least-squares and direct-computation methods. With a number of these methods, the analytical expression called the transfer function is obtained without first obtaining frequency-response data.

The Donegan-Pearson method requires a direct assumption as to the form of the transfer function and solves for the coefficients by substituting into the transfer function the input and the output time functions and their integrals. On the other hand, the exponential-approximation method solves for the coefficients of analytical expressions which approximate the time histories of the input and output functions. The transfer function is then established by taking the Laplace transform of these analytical functions.

In either the Donegan-Pearson or the exponential-approximation methods, the order of the expressions used to approximate either the transfer function or the input-output time histories is unlimited. Therefore, the requirement that the form of the transfer function be assumed would appear not to be particularly restrictive other than that the system be linear. In practice, however, the computation involved in the least-squares procedure increases rapidly with increase in the order of the equations and the equations tend to become progressively

more ill-conditioned. The general practice therefore has been to assume a form for a given transfer function, as would be predicted from the stability theory, and this practice, in general, neglects low-frequency (phugoid) modes and possible high-frequency modes due to structural elasticity in order to hold the order of the equations to a minimum. Such procedures do not afford detection of these modes from flight-test data in cases where these modes are important unless a form of the transfer function is assumed in advance which include such modes. In contrast, Fourier analysis will detect all details of the frequency response which are within the accuracy of the measurements and the calculation procedure. The forms of the longitudinal transfer functions usually assumed in conjunction with the curve-fitting methods are:

$$\left. \begin{aligned} \frac{\alpha}{\delta} &= \frac{E_p + F}{A_p^2 + B_p + C} \\ \frac{D\theta}{\delta} &= \frac{G_p + H}{A_p^2 + B_p + C} \\ \frac{n}{\delta} &= \frac{L_p^2 + M_p + N}{A_p^2 + B_p + C} \end{aligned} \right\} \quad (17)$$

where the substitution of $j\omega$ for the Laplace transform operator p gives the frequency response of the system.

Exponential-approximation methods.— Since the response of a linear system to a step or impulse is a sum of exponentials, an obvious method for fitting airplane time responses is the choice of exponential terms. The number of exponentials is selected so that the Laplace transformation will give the same polynomial expressions as obtained from stability theory. Although this method can be applied to any input that has a Laplace transform, it is most suited for application to responses to an approximate impulse, a step, and an approximate step input. The practical "approximate step," as compared to the theoretical perfect step, may have a small but finite lag in reaching steady state and may have a small undershoot or overshoot. (See ref. 16.) The response equation to a step may be represented for the case of the short-period longitudinal mode of motion of an airplane by the form

$$q(t) = q_{\infty} + e^{at}(J_1 \sin \omega t + J_2 \cos \omega t) \quad (18)$$

where a is the damping exponential, ω is the frequency, J_1 and J_2 are the coefficients of the in-phase and out-of-phase components of the response, and $q(t)$ is a function of time that expresses the response of the system.

In the Laplace transformation of the general form given by equation (18), the denominator of the transfer function would be given by

$$[p - (a + j\omega)][p - (a - j\omega)] = p^2 + bp + k \quad (19)$$

For lightly damped systems where the period and time to damp to one-half amplitude may be read directly from the response records, it has been found that direct calculation affords an accurate and rapid means of obtaining b and k . In the use of this method it follows from equations (18) and (19) that

$$b = \frac{1.386}{T_{1/2}} = -2a \quad (20)$$

$$k = \frac{0.48}{(T_{1/2})^2} + \frac{39.48}{P^2} = a^2 + \omega^2 \quad (21)$$

where $T_{1/2}$ is the time required for the oscillation to damp to one-half amplitude and P is the measured period of the oscillation.

This process, where the coefficients of the transfer function are computed from direct measurements of the flight records, has been used extensively for the case of rocket and free-fall test models since these test models, in general, exhibit the low damping and high natural frequency which enable this approach.

Once a and ω are determined, values of J_1 and J_2 appearing in equation (18) may be obtained from the time history. In instances where the steady state is adequately defined, direct computation of J_2 is afforded. In the analysis of the response of an airplane in angle of attack and pitching velocity over short periods of time, the coefficient J_2 must be negatively equal to the value of the response at

steady state. For the response in normal acceleration, however, a step input of the control surface causes an effective instantaneous change in load on the tail which, in turn, produces an instantaneous jump in the normal-acceleration response of the aircraft. An illustration of this type of response is shown in figure 4. The relationship among the instantaneous change in acceleration at $t = 0$, the steady-state acceleration, and J_2 is shown by equation (18) for $t = 0$ so that

$$q(0) = q_\infty + J_2 \quad (22)$$

With the coefficient J_2 thus established, a possibility for direct calculation of J_1 may be indicated for the case of a step input and lightly damped systems by writing equation (18) in the form

$$q(t) = q_\infty + e^{at} \sqrt{J_1^2 + J_2^2} \sin(\omega t + \phi) \quad (23)$$

and

$$\phi = \tan^{-1} \frac{J_2}{J_1} = \left(\frac{1}{2} - \frac{t_p}{P} \right) 2\pi \quad (24)$$

where P is the period of the oscillation and t_p is the time required for the oscillation to reach a peak after initiation of the step input. The relationship among ϕ , P , and t_p may be visualized by reference to figure 4.

The method of obtaining the transfer function for a system represented by equation (18) in response to a step input of the forcing function is shown in appendix C. The transfer function is of the form

$$\frac{Q}{\delta} (p) = \frac{\left(\frac{q_\infty + J_2}{\delta_0} \right) p^2 + \left(\frac{bq_\infty + J_1\omega - J_2a}{\delta_0} \right) p + \frac{kq_\infty}{\delta_0}}{p^2 + bp + k} \quad (25)$$

where a , b , k , and ω are related by equations (20) and (21), and δ_0 is the magnitude of the step.

As a general rule, the exponential-approximation method of simulating transient data seems to offer the best approach of any of the methods reported in this paper when the response is a lightly damped oscillation to an approximate step. It is of interest to note that this method may be used even though the input is not approximated by exponential expressions, provided its analysis is restricted to the free-oscillation portions of the response. The coefficients k , b , J_1 , and J_2 of equations (18) and (19) may be obtained regardless of the form of input provided that they are obtained from a portion of the time-response curve after the input has reached a steady-state value. This adaptation is pointed out by Shinbrot in reference 16 and the method of application is reported therein.

The foregoing method is useful only when the period and time to damp to one-half amplitude may be read directly from the records. For highly damped systems where this is not possible and as an alternate to the foregoing approach, a least-squares method for obtaining the period, damping, and other coefficients of equation (18) may be employed. Greenberg, in reference 4, discusses extensively the application of the Prony method for fitting a sum of exponentials to a number of equally spaced ordinates. This method will likewise obtain the transfer function given by equation (25).

A measure of how closely the analytical expression represents the time response of the system during free oscillation may be obtained by substituting the derived coefficients into equation (18) and allowing the time t to vary. This substitution amounts to taking the inverse Laplace transform of the transfer function, once it has been determined, and returning the function $Q(\omega)$ to the time domain where it should be equal to the original function of time $q(t)$.

The time required for this method varies with the number of least-squares solutions required to obtain the four unknowns b , k , J_1 , and J_2 . The extreme case is the case where a least-squares solution is desired for all the coefficients of a response. In this instance if the input is considered to be a step and the response is described by 24 data points, the time required to obtain the transfer function of the system may be estimated at 8 to 10 man-hours of work and three separate least-squares solutions are required. Any reduction in the number of least-squares solutions will obviously reduce the time required appreciably.

Donegan-Pearson method.- This method is appropriate for obtaining the transfer function from transient response to an arbitrary input, and, when only manual computing techniques are available, offers a good degree of accuracy with a minimum of work. The method is presented in

reference 17. In brief, a transfer function of one of the forms given by equation (17), for example,

$$(Ap^2 + Bp + C)q = \delta(Ep + F) \tag{26}$$

is integrated twice and rearranged to give

$$\frac{B}{A} \int_0^t q \, dt + \frac{C}{A} \int_0^t \int_0^T q \, dT \, dt - \frac{E}{A} \int_0^t \delta \, dt - \frac{F}{A} \int_0^t \int_0^T \delta \, dT \, dt = -q \tag{26a}$$

The equation is now in a form where the integrals may be calculated from q and δ which are known from a time history. The integral quantities in the foregoing equation are evaluated at some fixed time intervals, starting with the initial control input, to form a series of simultaneous equations from which the $\frac{B}{A}$, $\frac{C}{A}$, $\frac{E}{A}$, and $\frac{F}{A}$ coefficients may be evaluated by the least-squares method.

The expression of the transfer function in integral form is an important point with regard to application of this technique in that the integration processes are inherently more accurate than the differentiation process indicated in the normal form of the transfer functions. The integrals and the coefficients may be obtained by the matrix methods described in references 17 and 18. The use of higher-order terms in the numerator and denominator of the transfer function is possible but, in many cases, is unnecessary because of the insignificance of their coefficients and is impractical because of the large amount of additional work required.

In the derivation of this method no restriction is made or implied that the forcing function (input) or transient response reach a steady state within the time limit considered. There appears to be, however, a practical limitation on the length of the record since, for any given short length of a curve, a large number of analytical expressions may be written that satisfy, with good precision, the conditions of the curve in the region considered. Obviously, as the length of the record considered is extended, the expressions that adequately define the curve become more limited until the correct expression is closely approached. In the analysis of arbitrary inputs and responses that reached a steady state, this method produced excellent results over a large range of frequencies in a reasonably short length of time. When proficiency was

obtained in the use of this method, including the matrix methods of integration and least squares, a complete frequency response required about 8 man-hours of work from raw data (averaging about 20 data points) to finished frequency-response curves (averaging 16 frequencies).

In the application of this method, a somewhat simpler integrating matrix was used that reduced the time of integration by about one-half over the method presented in reference 17. The derivation of this integrating matrix by use of the relationships reported by Diederich in reference 18 is presented in appendix D.

A check on the accuracy with which the time response is represented is afforded by the inverse Laplace transformation process described in reference 3. A second method, which is suggested in reference 17, utilizes the evaluated integrals of the output, the recorded input, and the transfer function. If the transfer function is to represent the system accurately, the response obtained by this check must be equal to the original time response.

For both the Donegan-Pearson and exponential-approximation methods, a second approximation to the determined transfer-function coefficients may be made by a procedure suggested by Shinbrot in reference 16. In cases where this refining procedure was attempted, the process was lengthy and frequently did not afford better approximations because of failure of the method to converge.

RESULTS AND COMPARISONS OF METHODS

The frequency responses as obtained from three aircraft of different types are used herein for illustrative purposes. A summary of the mass and geometric parameters of these aircraft together with a sketch of their plan forms is presented in table I, as are the flight conditions for which the data were obtained. These aircraft will be referred to as a fighter, a transport, and a free-fall model.

All methods of analysis were not applied to all three of these aircraft, but a comparison of the methods is made herein for the fighter at one flight condition. The comparison is made with the response in pitching velocity to an elevator step input. Time histories of the control input and the response are shown in figure 5. The Donegan-Pearson, Prony, Fourier synthesizer, IBM, and manual Fourier methods were used to obtain the frequency response of the fighter from these time histories. A time interval of 0.10 second was used for the manual methods, 0.05 second was used for the IBM method, and 0.06 second was used for the Fourier synthesizer. The frequency-response curves thus obtained are shown in figure 6, together with the faired curve of figure 3 which was obtained

at the same flight conditions by the sinusoidal-response method. The frequency response of the fighter appears to be established to a generally acceptable degree by any one of the several methods shown. The expression "acceptable degree" is expanded subsequently.

Effect of Input Shape

Inasmuch as the compatibility of results obtained by using the various methods on a step input has been established, it is of interest to check the effect of this and other input shapes.

A check of the effect of input shape on results obtained through use of the Donegan-Pearson method has been made. The step input illustrated in figure 5 together with the approximately square and triangular inputs shown in figures 7 and 8, respectively, were used for the investigation and these inputs and their responses were analyzed at time intervals of 0.10 second. On each of these three figures, the accuracy with which the responses were represented by the transfer functions determined by the Donegan-Pearson method is shown by the data points on the response curve. These points represent values of pitching velocity obtained by multiplying the integrated functions of equation (26a) by the derived transfer coefficients at the values of time indicated in figure 5. This procedure is described in more detail in reference 17.

The frequency response of the fighter as determined by these transfer functions is shown in figure 9 compared with the faired curves of amplitude ratio and phase angle obtained from the sinusoidal-response method. The sinusoidal-response method is included because it involves a different test technique. These four sets of frequency-response curves appear to be in good agreement. Whether their agreement is to an "acceptable degree" may be illustrated by examining how closely they agree in the time domain when an identical control input is applied in each case. This process may be done manually through use of the inverse Laplace transformation; however, the Fourier synthesizer offers a machine method of obtaining the time response of a system described by the frequency-response curves to an approximate ramp or step. The Fourier synthesizer was used in the present analysis and the inverse of the process described in the section entitled "Description and Discussion of Methods" was applied.

The control input and time responses using the three frequency-response curves corresponding to the three input shapes investigated are shown in figure 10. The curves show a maximum spread about 13 percent of steady-state value at steady state and a smaller percentage spread at peak overshoot. Thus, it appears that the determination of the transfer function is not particularly sensitive to the shape of the control input when the Donegan-Pearson method is used.

Effect of Harmonic Content of Input

In the application of Fourier methods, the harmonic content of the input must be considered and has a predominant effect on the results obtained. Harmonic content pertains to the relative magnitudes of the sine waves of various frequencies which make up the input or response shape and is essentially the amplitude of the Fourier transform of a function.

In order to illustrate the harmonic content of several inputs, figure 11 shows the Fourier transforms of square, triangular, step, and impulse type of inputs plotted against frequency. It can be seen that the harmonic content of the square and triangular inputs go to zero at equally spaced increments of frequency, the spacing being dependent on the duration and shape of the input. For either shape, doubling the duration of the input will halve the spacing between the frequencies of zero harmonic content. An error frequently encountered in the frequency domain when Fourier methods are used is caused by the harmonic content of the Fourier transform of the input closely approaching or reaching zero. When this condition occurs, slight errors in the data cause the frequency-response curves to diverge and even to go to infinity at some frequency if the harmonic content of the input functions becomes zero at that frequency.

An example of the distortion of the frequency-response curves due to low harmonic content was obtained in the analysis by Fourier methods of the rectangular-pulse input and pitching-velocity response of the fighter as shown in figure 12. Because of the length of the rectangular-pulse input used, the harmonic content of both the input and response closely approached zero at frequencies of about 8.5 radians per second. The discontinuity due to the lack of harmonic content is shown in the frequency-response plot of figure 13. An additional test utilizing an input which affords data having good harmonic content in the region of uncertainty would be desirable in order to insure that no legitimate secondary peak or other significant characteristic exist in that range of frequencies.

When choosing inputs to be used in obtaining flight data for Fourier analysis, it is desirable to examine their harmonic amplitudes in light of expected instrument accuracies in order to select an input or series of inputs which will afford sufficiently accurate frequency-response data in the frequency range of interest.

Since it is desirable to maintain large values of harmonic content over the entire frequency range, inputs approaching an impulse would appear most usable. In practice, however, control inputs of this type having suitable amplitudes must be maintained over a significant length

of time so that the airplane is disturbed sufficiently to insure accurate measurement of the response. Thus, the transform of the resulting pulse will often closely approach or reach zero at some frequency in the range over which the response is desired.

The transform of the step input has the desirable feature of never becoming zero. Having infinite amplitude at zero frequency, the transform decreases as the inverse function of frequency and approaches zero amplitude as the frequency approaches infinity. In view of the rapid decrease in harmonic content with increase in frequency, however, it is sometimes difficult to maintain the accuracy of the frequency response to as high a value of frequency as desired. This effect may be seen in figure 11 by comparing the harmonic content of the triangular and step pulses from 1 to 8 radians per second.

The transforms of several basic inputs together with the effect on harmonic content of distortion of these basic inputs are illustrated in reference 10.

Effect of Record Length

The advantage indicated for the so-called curve-fitting methods with regard to their ability to make a logical interpolation over frequency regions of low harmonic content would also appear to be applicable to extrapolation in either the frequency or the time domain. For example, the fact that the analytical form of the transfer function is assumed in advance for these curve-fitting methods would appear to afford possibilities for analyzing only a part of an input and response to establish the coefficients of the transfer function whereas the Fourier analysis, by the nature of the limits of the Fourier integral, requires that a steady-state or a constant-amplitude oscillation be obtained. This apparent advantage of the curve-fitting methods in that the transient is not required to reach steady state has, in general, proven to have definite practical limitations. In the application of both Fourier and curve-fitting methods, it has been found that time transients that do not closely attain steady state do not produce accurate frequency-response data.

Figure 12, which shows the time history of a rectangular-pulse elevator input and the response in pitching velocity of the fighter, may be used to illustrate these practical limitations. The data were analyzed in three stages. The response was first considered in the time interval from $0 \leq t \leq 0.70$ second to be the response of the fighter to an approximate step where the pitching velocity appeared to reach a steady state before the elevator was again disturbed. Time increments of 0.05 second were used to obtain the frequency response of this portion of the time histories by the Prony, Donegan-Pearson, and manual Fourier methods.

(In this analysis, the Prony method required 16 man-hours; the Donegan-Pearson method required 9 man-hours.) In addition, check points were obtained by the manual Fourier method (by using Simpson's three-point rule of integration) with time intervals of 0.10, 0.025, and 0.0125 second. The frequency-response results of this analysis are shown in figure 14 and, although all the methods closely agree, the frequency response appears to be quite different from that indicated in figure 6 which was obtained for the same airplane at the same flight conditions.

The source of this discrepancy was determined when the time histories shown in figure 12 were again analyzed by using the Donegan-Pearson method at 0.05-second intervals to a time of 1.40 seconds where the response still had not approached a steady state too closely but the length of the record used had been doubled and the effective amplitude had been more than doubled. A third analysis was made by using the Donegan-Pearson method at 0.10-second intervals to 2.10 seconds at which time its steady-state value was closely attained. The frequency response obtained by using each of the three record lengths is shown in figure 15 together with the frequency response obtained for the fighter (by the Donegan-Pearson method) from figure 6. It may be seen that, when the first one-third of its response was analyzed, the record was short, and a steady state had not been reached; these factors precluded an adequately precise definition of the time response and an erroneous frequency response was obtained. When the length of the record was doubled, a more correct trend became apparent but, because a steady state had still not been defined, some fairly large discrepancies persisted, particularly with regard to the static value of the frequency response (the frequency-response curves of figure 6 being used as a basis for comparison). When the analysis included the entire response, even though the time interval used in the analysis was doubled, a close agreement with the frequency response obtained from the step input was obtained. Reference 17 recommends that enough of the response time history should be taken to cover the natural period of the system.

Other Causes and Effects of Errors

In the determination of transfer functions from inputs and outputs having regions of low harmonic content, an advantage has been indicated to the approach of fitting an analytical expression to experimental data. In the authors' opinion, this curve-fitting technique, as compared to the Fourier analysis, is of particular merit if there is reasonable confidence that the assumed analytical expression is of the correct form for the system being analyzed. In this manner, another condition (the form of the transfer function) is stipulated which the analysis must obey. In mathematical processes, the more conditions correctly stipulated, the more precise the results. On the other hand, errors in the transfer function or frequency response as obtained from the curve-fitting

methods due to either the wrong assumption of the form of the transfer function or due to the errors in the calculations are not readily apparent since the assumption of a given form will usually give variations that appear logical. However, as has been pointed out, certain checks, such as the use of the inverse Laplace transformation, are available for comparing the time response predicted from the transfer functions with the time-response curves from which the transfer functions were derived.

In the Fourier methods, inaccuracies are, in general, more readily discernible than in curve-fitting methods. In the use of Fourier methods, there has been found evidence of discrepancies attributable to three causes (as pointed out in ref. 10): the lack of harmonic content of the Fourier integral, the use of too large time intervals in the time domain to afford accuracy in the frequency domain, and the incorrect synchronization of input and response data in the time domain.

The first of these errors has already been discussed in the consideration of the effect of input on Fourier methods and, as has been pointed out, is usually discernible by divergence of the curves in some small range of frequencies.

The second of these errors, that of too large time intervals, is generally indicated by a scattering of the data points in the frequency domain where the magnitude of scatter usually diverges rapidly with increasing frequency. Insight into the cause of this scatter may be seen in the characteristics of the Fourier transform where, at each frequency, the transient $q(t)$ is multiplied by a sine and cosine wave of unit amplitude and where the resulting area under the two product curves determine the coefficients of the real and imaginary parts of the complex variable in the frequency domain. As frequencies greater than the natural frequency are investigated, the differences in the positive and negative areas of the product curves grow smaller (compared with the magnitude of the individual areas) so that the effect of small errors is magnified. Thus, small inaccuracies in the representation of the transient curve become more prominent as higher frequencies are investigated and appear in the frequency domain as scatter. Several estimates of the frequency at which scatter will become important, for the different Fourier methods, based on the time interval chosen, have been given in the section entitled "Description and Discussion of Methods."

A typical occurrence of scatter due to the choice of too large a time interval was obtained when the response of a free-fall model, the characteristics of which are given in table I, was analyzed at 0.10-second intervals by the manual Fourier (numerical-integration) method. The elevator input used and the response of the model in angle of attack are shown in figure 16. The frequency response as determined by the numerical manual Fourier, the Coradi harmonic analyzer, and the exponential-approximation methods of analysis are shown in figure 17. The scatter

of points obtained by the manual Fourier method of numerical integration occurs at frequencies greater than about 8 radians per second. Further analysis with smaller time intervals of, say, 0.05 second should provide better results in this region.

In the study of missiles and free-fall models where low damping is generally encountered, the use of the exponential-approximation method is particularly useful and requires a minimum of time. The response in figure 16 was analyzed by both the least-squares (Prony) method with 0.10-second intervals and by direct computation. Both gave identical coefficients and the frequency response obtained by using these coefficients is also shown in figure 17. The Donegan-Pearson method was attempted with this type of response but did not produce coefficients that represented this lightly damped system as exactly as it did for systems with high damping. The representation of the time response by the derived transfer function is illustrated in figure 16 where the inverse Laplace transform was applied to the transfer function obtained by the Donegan-Pearson and exponential-approximation methods to predict the response to a step. The reason for this condition is that the transfer coefficients which primarily determine the period and damping of the oscillation are determined by the double integration and integration, respectively, of the output. The smoothing effect of these integration processes on any existing oscillation does not therefore enable accurate detection of the oscillation characteristics.

Although scatter obtained by using the Fourier approach is indicative of inaccuracies, the converse does not apply inasmuch as the absence of scatter in the use of Fourier methods is not an indication of correctness. An illustration of this point was obtained in the analysis of the frequency response of the transport, tested under the conditions given in table I. The response in pitching velocity to an elevator input is shown in figure 18. The manual (numerical-integration) Fourier method, analyzed at 0.20-second intervals, was used to determine initially the response at 1, 3, 4, 5, and 8 radians per second and these frequency-response points are indicated in figure 19. Although the amplitude ratios and phase angles at the frequencies investigated did not indicate scatter, when two additional frequencies (6.5 and 7.5 radians per second) were investigated, the scatter became apparent. At a smaller time interval of 0.10 second, the control input and time response were analyzed by using the Fourier synthesizer, Donegan-Pearson, and again the manual (numerical integration) Fourier methods. Although small differences in the results are apparent in figure 19, they do agree sufficiently well for most purposes. A check point at a frequency of 8 radians per second and with a 0.05-second time interval was made with the numerical-integration Fourier method. The result essentially substantiated the value determined with 0.10-second time intervals.

The third mentioned cause of error often incurred in the Fourier analysis was referred to as incorrect synchronization of the input and response data in the time domain. A shift in the correlation of the time scales between input and output, in turn, causes a change in the phase angles obtained in the frequency domain by an amount directly proportional to the frequency. These erroneous values of lag or lead will be hard to detect regardless of whether Fourier or curve-fitting methods are used since incorrect but apparently logical frequency-response curves will usually occur.

In order to avoid or reduce errors in the determination of transfer functions from flight data, it is highly desirable to use as large a control deflection as possible, but the magnitude of this control deflection must also be compatible with the requirement that the stability parameters of the airplane remain within their linear range. It also appears highly desirable to analyze responses from two or more input shapes at a given flight condition. A comparison of the frequency response obtained from the same record by different methods has also proved a useful check.

As mentioned previously, examples indicating the times required to reduce flight data to frequency responses by the various methods discussed herein are summarized in table II. The table enables the weighing of the time factor in choice of a method; however, the choice depends on other factors as well, such as availability of machine computing equipment and limitations inherent in the various methods as have been discussed.

CONCLUDING REMARKS

In the foregoing study a number of considerations are indicated which pertain to the choice of methods in the determination of transfer functions and frequency response from transient data. These considerations may be summarized as follows:

In the methods which involve the analysis of transient responses over short periods of time, a control input should be used that will afford (a) a close approach to a steady-state condition and (b) response amplitudes and harmonic content (covering the frequency range of interest) large enough to give good instrument and reading accuracy yet small enough to keep the aircraft from departing from the flight condition for which the response data are desired. When flight data are analyzed, it appears highly desirable, as a check on the determined transfer function, to obtain responses from two or more input shapes at a given flight condition. A comparison of the frequency response obtained from the same record by different methods has also proved a useful check.

The method involving the oscillation of an aircraft through use of sinusoidal control inputs requires a large amount of flight time but a relatively simple analysis. Satisfactory data may be obtained with a human pilot generating an approximate sinusoidal control input. For modes of aircraft motion which are nearly critically damped, the large amount of flight time can be reduced somewhat since continuous records may be taken while the frequency of oscillation is slowly changed to cover the frequency range desired.

Two manual Fourier methods of analyzing arbitrary inputs and their responses were investigated. In the first approach, analytical expressions within discrete intervals are fitted to the time response and input, and terms of the Fourier integral are obtained analytically. In the second approach, the time response and input functions at selected times are first multiplied by the sine and cosine functions appearing in the Fourier integral and the resulting product curves are integrated numerically. The first approach appears to be basically more accurate when utilizing manual computing but is not as flexible or as suited to machine calculations as the second approach. Special machines for accomplishing a Fourier analysis, such as the Fourier synthesizer and Coradi harmonic analyzer, afford a means for significantly reducing calculation time as compared to a manual approach. The two machines mentioned give results comparable to those obtained by the usual manual procedure in numerical Fourier analyses. Because of its principle of operation, the Coradi harmonic analyzer appears to be basically more accurate than the Fourier synthesizer and, in general, gave satisfactory results out to somewhat higher frequencies. The Coradi harmonic analyzer appears more capable of handling random variations than the Fourier synthesizer. The mechanical application of the numerical Fourier analysis through use of punch-card calculating machines (for example, IBM equipment) is a means for appreciably reducing calculation time. This approach appears to afford the possibility of obtaining greater precision in the calculations since the rapid computation makes feasible the use of smaller time intervals combined with more complicated and precise integrating formulas.

The exponential-approximation and Donegan-Pearson methods establish an analytical expression for the transfer function which, in terms of the imaginary frequency variable, is continuous in frequency. The Fourier analysis, in contrast, does not furnish analytical expressions and gives values of frequency response only at selected frequencies. The Donegan-Pearson and Prony methods can be used satisfactorily when reasonable confidence exists as to the analytical forms of the transfer function (since the form must be assumed in advance). This approach will not, however, detect details of the frequency response that cannot be approximated by the assumed form even if such characteristics exist in the time response. In contrast, Fourier analysis will detect all details of the frequency

response which are within the accuracy of the measurements and the calculation procedure. The exponential-approximation method is best suited for lightly damped systems where the control input closely approximates a step or is of a form that possesses a simple Laplace transform. The longitudinal transfer functions of oscillatory aircraft can often be determined by simple, direct computation from the measured period, damping, steady-state value of the response, and phasing of the time response. Nonoscillatory transients that do not afford direct approximation of the response may be approximated by a least-squares procedure known as the Prony method. The Donegan-Pearson method appears best suited to systems that are not highly oscillatory and works well for inputs that are not necessarily represented by analytical expressions. When least-squares procedures must be applied in the Prony method, the Donegan-Pearson method generally affords shorter calculation time. When more than a few discrete frequencies are desired, the Donegan-Pearson method affords a more rapid approach than manual Fourier analysis.

Fourier methods are more critical to the forms of the input than the Donegan-Pearson method and inputs should be chosen to avoid regions of low harmonic content in the frequency range of interest. Although the Donegan-Pearson method appears to interpolate satisfactorily over regions of low harmonic content, it does not appear to be applicable to large extrapolation in either the frequency or time domain. In the use of this method, as in the Fourier methods, it is necessary to obtain data which closely approach the steady state in order to predict accurately the low-frequency-response characteristics.

Langley Aeronautical Laboratory,
National Advisory Committee for Aeronautics,
Langley Field, Va., June 4, 1953.

APPENDIX A

ESTIMATION OF THE ERRORS ENCOUNTERED USING A CONTROL INPUT
 THAT CHANGES IN FREQUENCY AT A CONSTANT RATE

Much of the extensive flight-test time involved in obtaining frequency-response data by using a sinusoidal input can be eliminated if the sinusoidal input is continuously changed in frequency at a slow rate. Since transients are constantly being introduced and dying out because of this constantly changing frequency, the error introduced by assuming that the response to this wave approximates the steady-state response to a constant-frequency wave may, at any given frequency, be a function of the natural frequency and damping of the airplane as well as the rate at which the frequency is changed. Investigation of the magnitudes of these errors in amplitude and phase angle based on the response of the airplane to a constant-frequency sinusoidal input was performed as follows:

If a wave form of constant amplitude and constantly changing frequency is compared with a sinusoidal wave form having the same amplitude but constant frequency, there will occur, at a time herein assumed to be zero, a condition where the amplitude and instantaneous frequency of the two waves will be identical. In the following derivation, the frequency at this instant is defined as ω_0 and the two waves are adjusted so that at this instant both waves are at their maximum amplitude. A second-order system is considered. The differential equation relating the response of the system to a constant frequency input is then

$$\left(\frac{D^2}{\omega_n^2} + \frac{2\zeta}{\omega_n} D + 1 \right) x = \cos \omega_0 t \quad (A1)$$

Similarly, for the varying cosine wave, this differential equation is

$$\left(\frac{D^2}{\omega_n^2} + \frac{2\zeta}{\omega_n} D + 1 \right) x = \cos(\omega_0 + Ct)t \quad (A2)$$

Comparison of the two inputs show that their difference is effectively a phase difference which varies as the parabola $\phi = Ct^2$. Since

a time-response solution of equation (A2) was too cumbersome to be feasible, a linear-phase relationship was chosen that would approximate the parabolic-phase relationship and would afford a relatively simple time-response solution. A wave having a linear-phase difference with a constant-frequency wave is, of course, another constant-frequency wave of a different frequency. Although a constant-frequency wave would not appear to be a good approximation to the variable-frequency wave under consideration, it will be shown that the difference between the original constant-frequency wave and the varying-frequency wave may be closely approximated by the difference between the two constant-frequency waves within the region of interest provided their frequencies are properly selected.

The procedure used for establishing the frequency of the wave used in the approximation, in terms of the rate of change of frequency of the variable-frequency wave, is as follows: The actual phase-angle variation and the assumed approximation are illustrated in figure 20. The time interval over which the actual phase-angle variation was approximated was the interval which would enable transients introduced by the varying-frequency wave to reduce to one-twentieth of their initial value ($-T_{1/20} \leq t \leq 0$). The parabola was approximated by a straight line chosen to pass through the parabola at the times $t = 0$ and $t = -\frac{2}{3} T_{1/20}$. The approximation was chosen to balance the areas between the parabola and the straight line in the region of interest. Substitution of the approximate phase angle into the varying-frequency input for the right-hand side of equation (A2) gives

$$\cos\left(\omega_0 - \frac{2}{3} C T_{1/20}\right)t \tag{A3}$$

The relationships $T_{1/20} = \frac{3}{\zeta\omega_n}$ and $D\omega = \frac{d^2}{dt^2}(\omega_0 t + Ct^2) = 2C$ may be substituted into equation (A3) to give

$$\cos\left(\omega_0 - \frac{D\omega}{\zeta\omega_n}\right)t \tag{A4}$$

For an example case where $D\omega = 1$ radian per second per second and $\omega_0 = 8$ radians per second, the original constant-frequency wave (eq. (A1)) and the varying-frequency wave (eq. (A2)) are shown in figure 21 together with the wave used to approximate the phase-angle relationship between the original two (eq. (A4)). In addition, the difference between the original constant-frequency wave and the varying-frequency wave is compared in figure 21 with the difference between the original constant-frequency wave and the wave used in the approximation of the phase-angle relationship.

The errors in phase and amplitude incurred in the response of the second-order system and caused by the use of a varying-frequency-wave input instead of a constant-frequency-wave input may be obtained by determining the difference between the phase angles and amplitude ratios obtained from these two inputs. These errors are given by

$$x_e = \frac{\cos \omega_0 t}{\frac{D^2}{\omega_n^2} + \frac{2\zeta}{\omega_n} D + 1} - \frac{\cos \left(\omega_0 - \frac{D\omega}{\zeta\omega_n} \right) t}{\frac{D^2}{\omega_n^2} + \frac{2\zeta}{\omega_n} D + 1} \quad (A5)$$

The substitution of $D = j\omega_0$ for the response to $\cos \omega_0 t$ and the substitution of $D = j \left(\omega_0 - \frac{D\omega}{\zeta\omega_n} \right)$ for the response to $\cos \left(\omega_0 - \frac{D\omega}{\zeta\omega_n} \right) t$ will, at $t = 0$, give the error relationship in terms of amplitude and phase angle

$$|x_e(0)| = \frac{1}{\sqrt{\left[1 - \left(\frac{\omega_0}{\omega_n} \right)^2 \right]^2 + \left[2\zeta \left(\frac{\omega_0}{\omega_n} \right) \right]^2}} - \frac{1}{\sqrt{\left[1 - \left(\frac{\omega_0}{\omega_n} - \frac{D\omega}{\zeta\omega_n^2} \right)^2 \right]^2 + \left[2\zeta \left(\frac{\omega_0}{\omega_n} - \frac{D\omega}{\zeta\omega_n^2} \right) \right]^2}}$$

$$\phi_e = -\tan^{-1} \frac{2\zeta \frac{\omega_0}{\omega_n}}{1 - \left(\frac{\omega_0}{\omega_n} \right)^2} + \tan^{-1} \frac{2\zeta \left(\frac{\omega_0}{\omega_n} - \frac{D\omega}{\zeta\omega_n^2} \right)}{1 - \left(\frac{\omega_0}{\omega_n} - \frac{D\omega}{\zeta\omega_n^2} \right)^2}$$

Various values of damping ratio ζ , frequency ratio ω_0/ω_n , and the rate of change of frequency ratio $D\omega/\omega_n^2$ were substituted into the foregoing relations in order to obtain plots of phase error and amplitude error (related to the response to a pure sinusoidal input) at zero time. Figure 22 presents plots of these errors over a range of values of parameters pertinent to most aircraft. This figure indicates that the errors increase rapidly with a decrease in the value of damping ratio below 0.707. At low values of damping ratio, excessively large errors will be obtained unless the frequency is varied at an extremely low rate in the vicinity of $\frac{D\omega}{\omega_n^2} = 0.01$. The greatest errors in all cases appear to occur in the vicinity of the natural frequency, the errors approaching zero at high and low values of the frequency ratio.

For the tests presented in the body of this paper, the airplane tested had a damping ratio of about 0.7. The rate of change of frequency for these tests was not constant but rather was held constant at one frequency for several oscillations before progressing to a new frequency. However, averaging over a range of frequencies gave an average value of $D\omega/\omega_n^2$ of 0.06. Figure 22 indicates an error in amplitude and in phase angle of less than 10 percent for the airplane tested at these conditions. This error falls within the scatter shown in figure 3.

APPENDIX B

METHODS OF FOURIER ANALYSIS WHEREIN THE TRANSIENTS
 ARE REPRESENTED BY A SERIES OF POLYNOMIALS

A representation of an approximate step-control input and the time response of pitching velocity of the fighter as shown in figure 5 involved the division of the input into three intervals of time and the division of the response into five intervals of time.

The input, which reaches a steady-state value of -0.74° at $t = 0.10$ second, was represented within the intervals by the equations

$$\delta_0(t) = 20t^2 \quad (0 \leq t \leq 0.05)$$

$$\delta_1(t) = 13.8t - 0.64 \quad (0.05 \leq t \leq 0.10)$$

$$\delta_2(t) = 0.74 \quad (0.10 \leq t \leq \infty)$$

The Fourier transform of the input is then

$$\delta(\omega) = 20 \int_0^{0.05} t^2 e^{-j\omega t} dt + \int_{0.05}^{0.10} (13.8t - 0.64) e^{-j\omega t} dt +$$

$$0.74 \int_{0.10}^{\infty} e^{-j\omega t} dt$$

$$= \frac{13.8e^{-0.10j\omega} - 11.8e^{-0.05j\omega}}{\omega^2} + j \frac{40(1 - e^{-0.05j\omega})}{\omega^3}$$

or in trigonometric form

$$\delta(\omega) = \frac{13.8}{\omega^2} \cos 0.10\omega - \frac{11.8}{\omega^2} \cos 0.05\omega - \frac{40}{\omega^3} \sin 0.05\omega +$$

$$j \left[\frac{11.8}{\omega^2} \sin 0.05\omega - \frac{13.8}{\omega^2} \sin 0.10\omega + \frac{40}{\omega^3} (1 - \cos 0.05\omega) \right] \quad (B1)$$

where the substitution of selected values of frequency ω will afford the real and imaginary coefficients of the Fourier transform at each frequency chosen.

The time response of pitching velocity, shown in figure 5, was divided into discrete intervals and the coefficients of the cubic equation

$$D\theta(t) = at^3 + bt^2 + ct + d$$

were found as follows:

For the time interval $0 \leq t \leq 0.10$, inspection of the curve indicates that it may be closely approximated by a cubic without lower-order terms so that $b = c = d = 0$ and, at $t = 0.10$ second, the relationship is written

$$D\theta(t) = at^3$$

$$0.0049 = a(0.10)^3$$

$$4.9 = a$$

The equation for this time interval becomes

$$D\theta_0(t) = 4.9t^3$$

For the time interval $0.10 \leq t \leq 0.30$, a quadratic representation, since the transient in this interval does not indicate the need of a cubic representation, will be assumed where the coefficients are found by the solution of the following equations:

$$D\theta(t = 0.10) \quad 0.0049 = (0.10)^2 b + (0.10)c + d$$

$$D\theta(t = 0.20) \quad 0.0489 = (0.20)^2 b + (0.20)c + d$$

$$D\theta(t = 0.30) \quad 0.0733 = (0.30)^2 b + (0.30)c + d$$

The solution by "successive subtraction" is illustrated here since equal time intervals were used.

$$0.0049 - 0.0489 = (0.01 - 0.04)b + (0.10 - 0.20)c + \cancel{(1 - 1)d} \rightarrow 0$$

$$0.0489 - 0.0733 = (0.04 - 0.09)b + (0.20 - 0.30)c + \cancel{(1 - 1)d} \rightarrow 0$$

$$0.0440 = 0.03b + 0.10c$$

$$0.0244 = 0.05b + 0.10c$$

$$0.0440 - 0.0244 = (0.03 - 0.05)b + \cancel{(0.10 - 0.10)c} \rightarrow 0$$

$$0.0196 = -0.02b$$

$$-0.98 = b$$

$$0.734 = c$$

$$-0.0587 = d$$

The equation for this time interval becomes

$$D\theta_1(t) = -0.98t^2 + 0.734t - 0.0587$$

For the time interval $0.30 \leq t \leq 0.80$, the slope of the transient is zero at a time of 0.55 second. Use of this condition is desirable in evaluating the constants over this interval; therefore,

$$D\theta(t = 0.30) \quad 0.0733 = (0.30)^3 a + (0.30)^2 b + (0.30)c + d$$

$$D\theta(t = 0.55) \quad 0.0856 = (0.55)^3 a + (0.55)^2 b + (0.55)c + d$$

$$D\theta(t = 0.80) \quad 0.0793 = (0.80)^3 a + (0.80)^2 b + (0.80)c + d$$

$$D^2\theta(t = 0.55) \quad 0 = 3(0.55)^2 a + 2(0.55)b + c$$

and the equation for this time interval becomes

$$D\theta_2(t) = 0.192t^3 - 0.4655t^2 + 0.3379t + 0.00862$$

For the time interval $0.80 \leq t \leq 1.40$, the solution of

$$D\theta(t = 0.80) \quad 0.0793 = (0.80)^3 a + (0.80)^2 b + (0.80)c + d$$

$$D\theta(t = 1.00) \quad 0.0723 = (1.00)^3 a + (1.00)^2 b + (1.00)c + d$$

$$D\theta(t = 1.20) \quad 0.0665 = (1.20)^3 a + (1.20)^2 b + (1.20)c + d$$

$$D\theta(t = 1.40) \quad 0.0636 = (1.40)^3 a + (1.40)^2 b + (1.40)c + d$$

gives an equation for this time interval of

$$D\theta_3(t) = 0.0354t^3 - 0.09125t^2 + 0.0425t + 0.08565$$

For the time interval $1.40 \leq t \leq \infty$, the equation for a constant value from steady state to infinity becomes

$$D\theta(t = 1.40) \quad 0.0636 = d$$

Therefore,

$$D\theta_4(t) = 0.0636$$

The Fourier transform of the response is now evaluated by using the foregoing analytical expressions by summing the following integrals:

$$\begin{aligned} D\theta(\omega) &= \int_0^{\infty} D\theta(t) e^{-j\omega t} dt \\ &= 4.9 \int_0^{0.10} t^3 e^{-j\omega t} dt - \int_{0.10}^{0.30} (0.98t^2 - 0.734t + 0.0587) e^{-j\omega t} dt + \\ &\quad \int_{0.30}^{0.80} (0.192t^3 - 0.4655t^2 + 0.3379t + 0.00862) e^{-j\omega t} dt + \\ &\quad \int_{0.80}^{1.40} (0.0354t^3 - 0.09125t^2 + 0.0425t + 0.08565) e^{-j\omega t} dt + \\ &\quad 0.0636 \int_{1.40}^{\infty} e^{-j\omega t} dt \end{aligned}$$

The integration of these terms (given in text after eq. (6)) leads to the following relations:

$$\begin{aligned}
 D\theta(\omega) = & \frac{58.8}{\omega^4} - \frac{1}{\omega^2} \left[\left(\frac{58.8}{\omega^2} - 0.391 \right) + j \left(\frac{4.9}{\omega} \right) \right] (\cos 0.10\omega - j \sin 0.10\omega) + \\
 & \frac{1}{\omega^2} \left[\left(\frac{2.305}{\omega^2} + 0.0358 \right) + j \left(\frac{1.375}{\omega} \right) \right] (\cos 0.30\omega - j \sin 0.30\omega) - \\
 & \frac{1}{\omega^2} \left[\left(\frac{1.88}{\omega^2} + 0.0031 \right) - j \left(\frac{0.0035}{\omega} \right) \right] (\cos 0.80\omega - j \sin 0.80\omega) - \\
 & \frac{1}{\omega^2} \left[\left(\frac{0.4248}{\omega^2} + 0.0047 \right) + j \left(\frac{0.1149}{\omega} \right) \right] (\cos 1.40\omega - j \sin 1.40\omega) \quad (B2)
 \end{aligned}$$

where the substitution of selected values of ω affords the real and imaginary coefficients of the Fourier transform of the pitching-velocity response of the fighter. The relationship between the output and the input is given by equations (4), (6), and (7) and a plot of these relationships at several values of frequency are shown in figure 6.

APPENDIX C

APPLICATION OF THE LAPLACE TRANSFORM TO A RESPONSE EQUATION

The response equation for the normal acceleration, as used in the Prony method described by Greenberg in reference 4, is

$$n(t) = n_{ss} + e^{at}(J_1 \sin \omega t + J_2 \cos \omega t) \quad (C1)$$

where n_{ss} is the normal acceleration at steady state. The equation for a step control input of magnitude δ_0 is as follows:

$$\delta(t) = \delta_0 \quad (t \geq 0) \quad (C2)$$

The Laplace transform, indicated by the operator p when applied to equation (C1), gives

$$n(p) = \frac{n_{ss}}{p} + \frac{J_1 \omega}{(p - a)^2 + \omega^2} + \frac{J_2(p - a)}{(p - a)^2 + \omega^2} \quad (C3)$$

and equation (C2) becomes

$$\delta(p) = \frac{\delta_0}{p} \quad (C4)$$

By definition, the transfer function is the ratio of the Laplace transform of the output to the Laplace transform of the input (initial conditions zero)

$$\begin{aligned} \frac{n(p)}{\delta(p)} &= \frac{1}{\delta_0} \left[n_{ss} + \frac{J_1 \omega p + J_2 p(p - a)}{p^2 - 2ap + a^2 + \omega^2} \right] \\ &= \frac{1}{\delta_0} \left[n_{ss} + \frac{J_2 p^2 + (J_1 \omega - J_2 a)p}{p^2 + bp + k} \right] \end{aligned} \quad (C5)$$

where the substitution of $b = -2a$ and $k = a^2 + \omega^2$ has been made. The equation may be rearranged to agree with the form of equations (17) so that

$$\frac{n}{\delta}(p) = \frac{p^2 \frac{n_{ss} + J_2}{\delta_0} + p \frac{bn_{ss} + J_1\omega - J_2a}{\delta_0} + \frac{kn_{ss}}{\delta_0}}{p^2 + bp + k} \quad (C6)$$

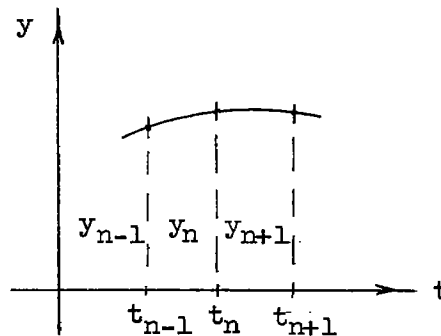
where the substitution of $j\omega$ for the operator p will produce the frequency-response relationships.

APPENDIX D

AN INTEGRATING MATRIX

The Donegan-Pearson method (ref. 17) of analysis of transient responses suggests a matrix solution which, if followed, requires some knowledge of integrating matrices. An integrating matrix believed to be somewhat easier to use than the one suggested in reference 17 is presented here together with its derivation.

If an arbitrary time-curve is chosen and divided into equal intervals of time, then by Simpson's rule a parabola may be described through three adjoining points



By the use of equation (A4) of reference 18,

$$\int_{t_{n-1}}^{t_n} y \, dt = \left(\frac{5}{12} \Delta t\right) y_{n-1} + \left(\frac{2}{3} \Delta t\right) y_n + \left(-\frac{1}{12} \Delta t\right) y_{n+1} \quad (D1)$$

Solution of equation (D1) for values of the integers $n = 0, 1, 2, 3, 4, \dots, m$ gives

$$\int_{t_{n-1}}^{t_n} y \, dt = 0 \quad (n = 0)$$

$$\int_{t_{n-1}}^{t_n} y \, dt = \frac{\Delta t}{12} (5y_{n-1} + 8y_n - y_{n+1}) \quad (n = 1)$$

$$\int_{t_{n-1}}^{t_n} y \, dt = \frac{\Delta t}{12} (5y_{n-2} + 13y_{n-1} + 7y_n - y_{n+1}) \quad (n = 2)$$

$$\int_{t_{n-1}}^{t_n} y \, dt = \frac{\Delta t}{12} (5y_{n-3} + 13y_{n-2} + 12y_{n-1} + 7y_n - y_{n+1}) \quad (n = 3)$$

$$\int_{t_{n-1}}^{t_n} y \, dt = \frac{\Delta t}{12} (5y_{n-4} + 13y_{n-3} + 12y_{n-2} + 12y_{n-1} + 7y_n - y_{n+1}) \quad (n = 4)$$

$$\int_{t_{n-1}}^{t_n} y \, dt = \frac{\Delta t}{12} (5y_{n-m} + 13y_{n-(m-1)} + 12y_{n-(m-2)} + \dots + 12y_{n-1} + 7y_n - y_{n+1}) \quad (n = m)$$

Written in tabular form (without fixing a value for Δt), the coefficients of y appear in the integrating matrix in the form

t	0	Δt	$2 \Delta t$	$3 \Delta t$	$4 \Delta t$	$5 \Delta t$	$6 \Delta t$	$7 \Delta t$
0	0	0	0	0	0	0	0	0
Δt	0.416667 Δt	0.666667 Δt	-0.083333 Δt	0	0	0	0	0
$2 \Delta t$.416667 Δt	1.083333 Δt	.583333 Δt	-0.083333 Δt	0	0	0	0
$3 \Delta t$.416667 Δt	1.083333 Δt	1.000000 Δt	.583333 Δt	-0.083333 Δt	0	0	0
$4 \Delta t$.416667 Δt	1.083333 Δt	1.000000 Δt	1.000000 Δt	.583333 Δt	-0.083333 Δt	0	0
$5 \Delta t$.416667 Δt	1.083333 Δt	1.000000 Δt	1.000000 Δt	1.000000 Δt	.583333 Δt	-0.083333 Δt	0
$6 \Delta t$.416667 Δt	1.083333 Δt	1.000000 Δt	1.000000 Δt	1.000000 Δt	1.000000 Δt	.583333 Δt	-0.083333 Δt

The use of this integrating matrix simply requires the accumulative summation of---

$$(0.416666 \Delta t)y_{n-1} + (0.666666 \Delta t)y_n - (0.083333 \Delta t)y_{n+1}$$

which gives the area lying between $n - 1$ and n added to the area already found from 0 to $n - 1$.

REFERENCES

1. Bollay, William: Aerodynamic Stability and Automatic Control. Jour. Aero. Sci., vol. 18, no. 9, Sept. 1951, pp. 569-617.
2. Milliken, W. F., Jr.: Dynamic Stability and Control Research. Rep. No. Cal-39, Cornell Aero. Lab., Inc., (Presented at Third International Joint Conference of the R.A.S.-I.A.S., Brighton, England, Sept. 3-14, 1951.)
3. Gardner, Murray F., and Barnes, John L.: Transients in Linear Systems Studied by the Laplace Transformation. Lumped-Constant Systems. Vol. I, John Wiley & Sons, Inc., 1942.
4. Greenberg, Harry: A Survey of Methods for Determining Stability Parameters of an Airplane From Dynamic Flight Measurements. NACA TN 2340, 1951. ✓
5. Lees, Sidney: Graphical Aids for the Graphical Representation of Functions of the Imaginary Argument. M.I.T., Instrumentation Lab., Engineering Memo. E-25, Feb. 1951.
6. Jones, Robert T., and Sternfield, Leonard: A Method for Predicting the Stability in Roll of Automatically Controlled Aircraft Based on the Experimental Determination of the Characteristics of an Automatic Pilot. NACA TN 1901, 1949.
7. LaVerne, Melvin E., and Boksenbom, Aaron S.: Frequency Response of Linear Systems From Transient Data. NACA Rep. 977, 1950. (Supersedes NACA TN 1935.) ✓
8. Schetzer, J. D.: Notes on Dynamics for Aerodynamicists. Rep. No. SM-14077, Douglas Aircraft Co., Inc., Nov. 19, 1951. ✓
9. Milne, William Edmund: Numerical Calculus. Princeton Univ. Press, 1949.
10. Breaux, G. P., and Zeiller, E. L.: Dynamic Response Program on the B-36 Airplane: Part III - Presentation and Theoretical Considerations of the Transient Analysis Method Employed for Obtaining Frequency Response Functions From Flight Data. Rep. No. FZA-36-195, Consolidated Vultee Aircraft Corp., Feb. 14, 1952.
11. Seamans, R. C., Jr., Blasingame, B. P., and Clementson, G. C.: The Pulse Method for the Determination of Aircraft Dynamic Performance. Jour. Aero. Sci., vol. 17, no. 1, Jan. 1950, pp. 22-38. ✓

12. Seamans, Robert C., Jr., Bromberg, Benjamin G., and Payne, L. E.: Application of the Performance Operator to Aircraft Automatic Control. Jour. Aero. Sci., vol. 15, no. 9, Sept. 1948, pp. 535-555.
13. Curfman, Howard J., Jr., and Gardiner, Robert A.: Method for Determining the Frequency-Response Characteristics of an Element or System From the System Transient Output Response to a Known Input Function. NACA Rep. 984, 1950. (Supersedes NACA TN 1964.)
14. Lipka, Joseph: Graphical and Mechanical Computation. John Wiley & Sons, Inc., 1918.
15. Miller, Dayton C.: The Henrici Harmonic Analyzer and Devices for Extending and Facilitating Its Use. Jour. Franklin Inst., vol. 182, no. 3, Sept. 1916, pp. 285-322.
16. Shinbrot, Marvin: A Least Squares Curve Fitting Method With Applications to the Calculation of Stability Coefficients From Transient-Response Data. NACA TN 2341, 1951.
17. Donegan, James J., and Pearson, Henry A.: Matrix Method of Determining the Longitudinal-Stability Coefficients and Frequency Response of an Aircraft From Transient Flight Data. NACA Rep. 1070, 1952. (Supersedes NACA TN 2370.)
18. Diederich, Franklin W.: Calculation of the Aerodynamic Loading of Swept and Unswept Flexible Wings of Arbitrary Stiffness. NACA Rep. 1000, 1950. (Supersedes NACA TN 1876.)

TABLE I
 CHARACTERISTICS AND FLIGHT CONDITIONS OF AIRCRAFT
 USED FOR LONGITUDINAL TESTS

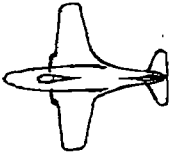
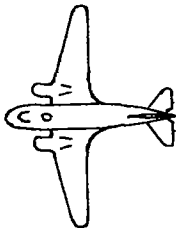

Condition	 Fighter	 Transport	 Free-fall model
Weight, lb	12,840	23,000	1,030
Tail length, ft	16.0	37.0	3.7
Wing area, sq ft	250	988.9	9.0
Horizontal tail area, sq ft	66.2	179.2	1.72
Aspect ratio	4.975	9.13	4.0
Wing span, ft	35.25	95.0	6.0
Mean aerodynamic chord, ft	7.45	11.5	1.5312
Pressure attitude, ft	10,000	5,000	32,000
Mach number	0.60	0.268	0.725
Moment of inertia in pitch, slug-ft ²	17,311	91,690	50
Sweep, deg	0	15.5	45.0
Aircraft density factor	122.0	30.6	2,730

TABLE II
EXAMPLES OF TIMES REQUIRED TO OBTAIN FREQUENCY DATA
FROM TRANSIENT DATA BY VARIOUS METHODS

Method of analysis	Number of functions analyzed	Number of data points per function	Number of frequencies analyzed per function	Time required to obtain transfer functions, hr	Time required to obtain frequency response, hr
Sinusoidal	2	---	16	-----	2
Fourier:					
Analytical integration	2	15	11	-----	12
Numerical integration	2	24	8	-----	12
Punch-card computer (IBM)	2	241	12	-----	10
Fourier synthesizer	2	24	^a 12	-----	4 to 8
Coradi harmonic analyzer	2	Continuous curve	10	-----	8
Curve fitting:					
Exponential approximation					
Direct computation	^b 1	24	^a 15	0.5	2.5
Prony	^b 1	24	^a 15	6 to 8	8 to 10
Donegan-Pearson	2	20	^a 16	6	8

^aResults were obtained in form continuous with frequency but numerical evaluation was made at number of frequencies shown.

^bMethod is primarily applicable to impulse or step inputs; therefore, analysis of the input function is not required.



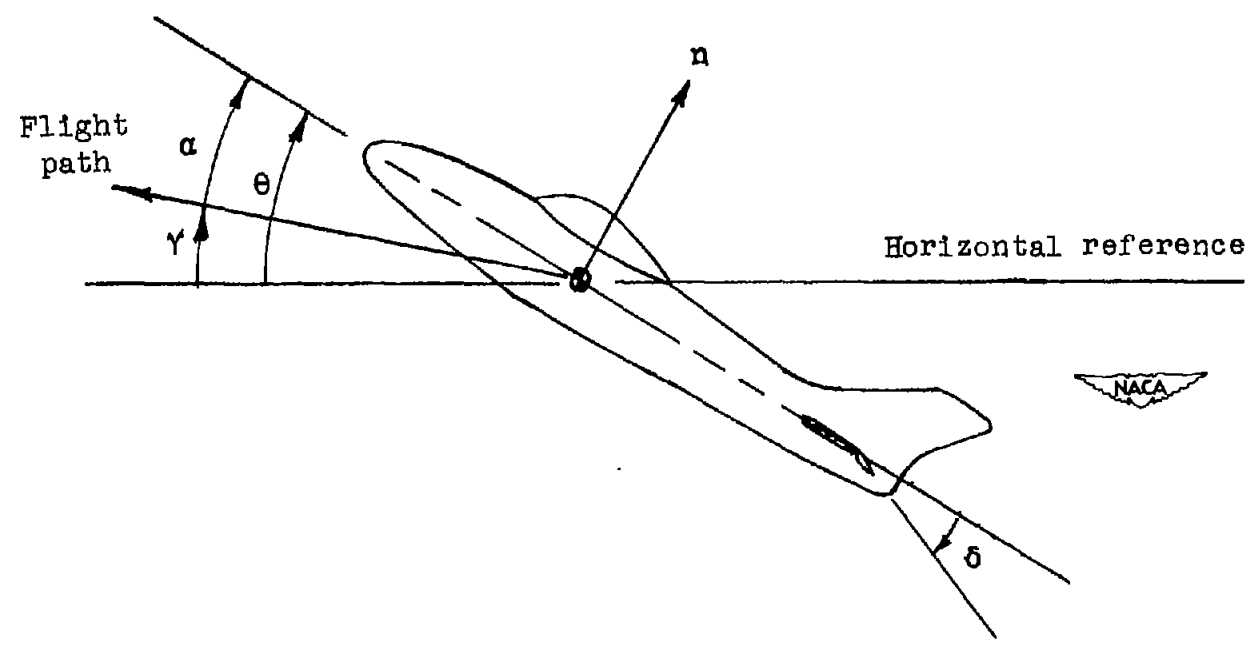


Figure 1.- Sign convention. Arrows indicate positive direction.

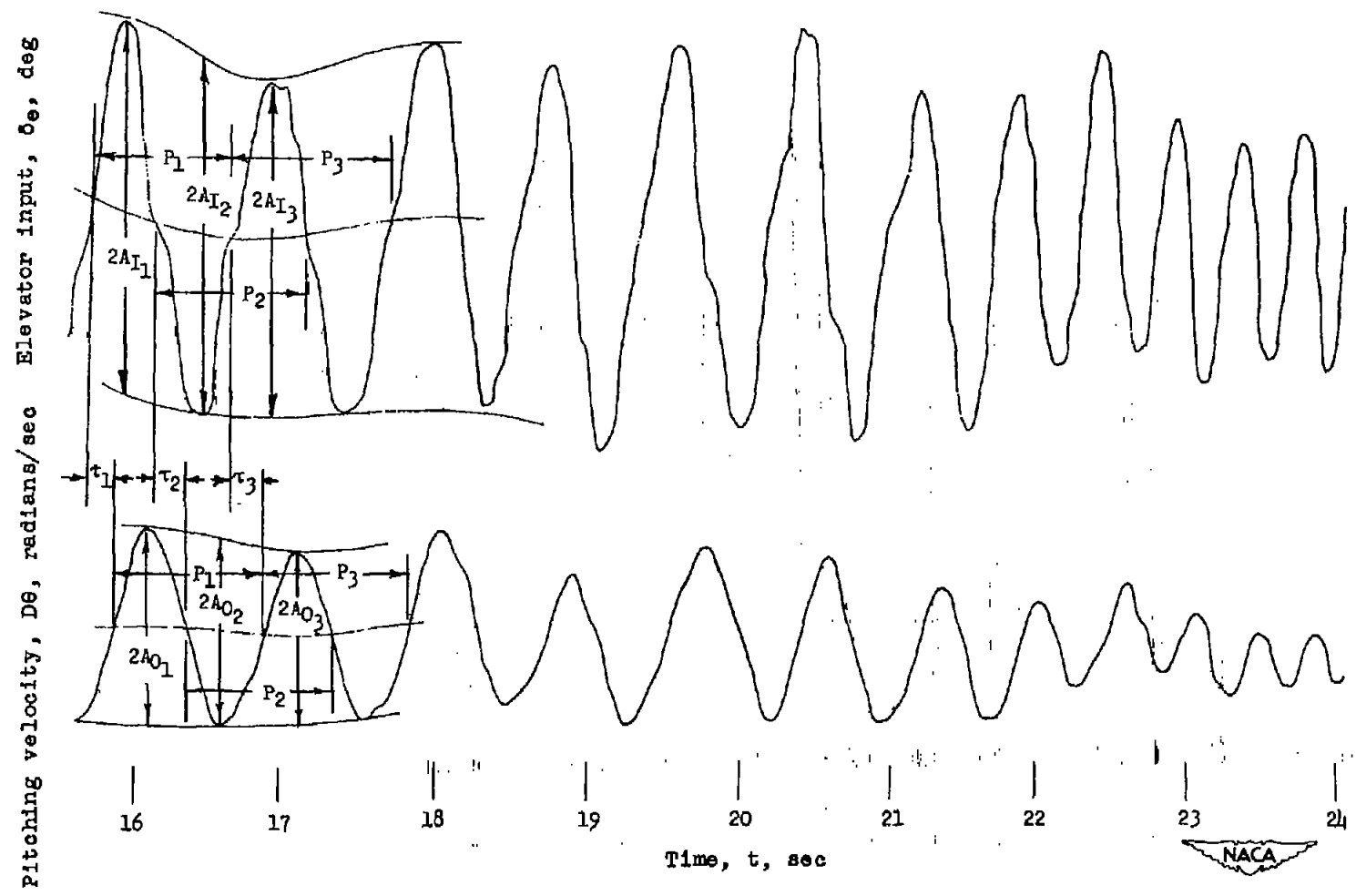


Figure 2.- Film records of sinusoidal elevator input and response of fighter in pitching velocity at $M = 0.6$ and $h_p = 10,000$ feet.
 Average amplitude, $\frac{1}{3} (A_1 + A_2 + A_3)$; average period, $\frac{1}{3} (P_1 + P_2 + P_3)$;
 average lag, $\frac{1}{3} (\tau_1 + \tau_2 + \tau_3)$.



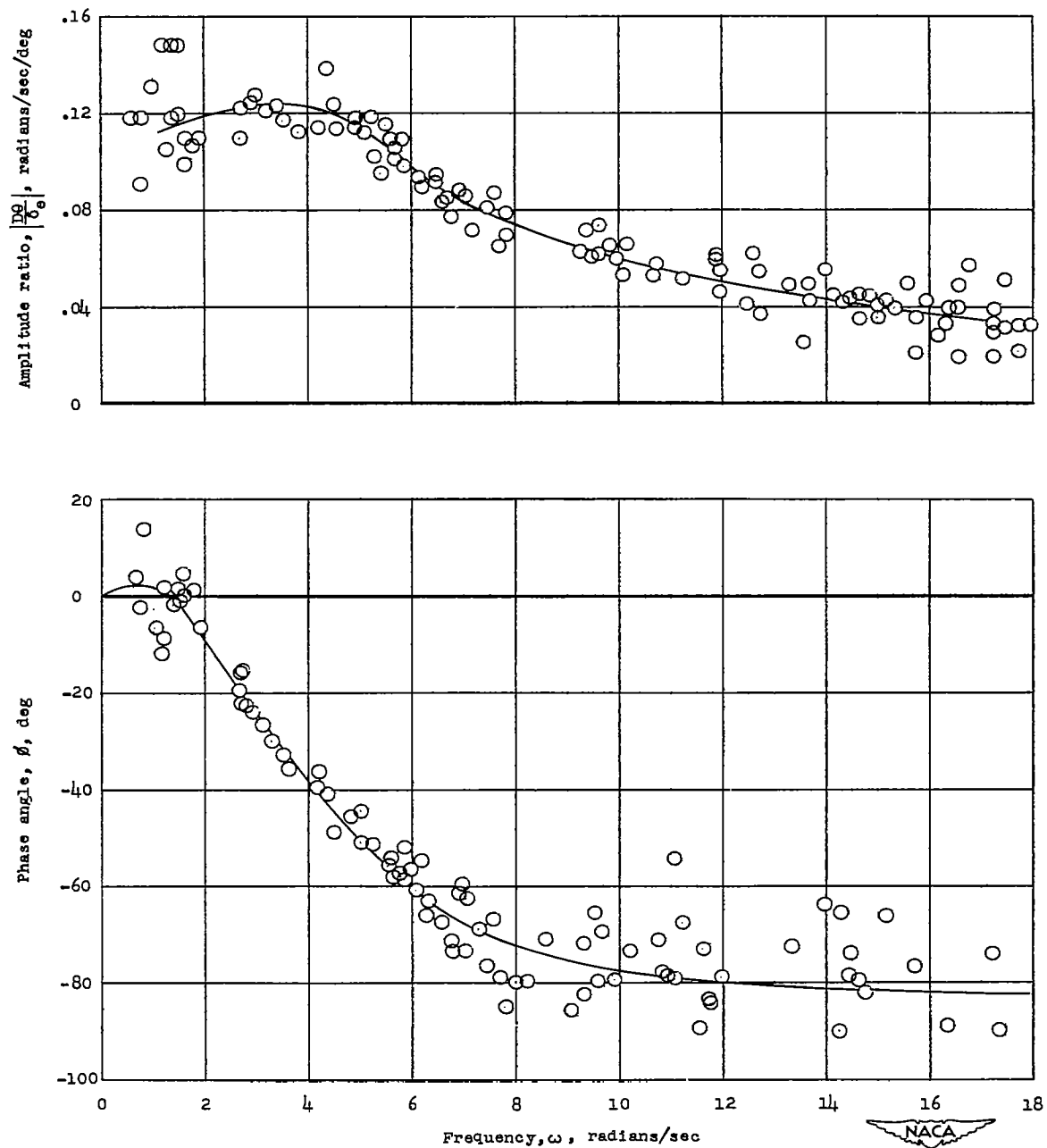


Figure 3.- Sinusoidal-response data points of fighter airplane at $M = 0.6$ and $h_p = 10,000$ feet.

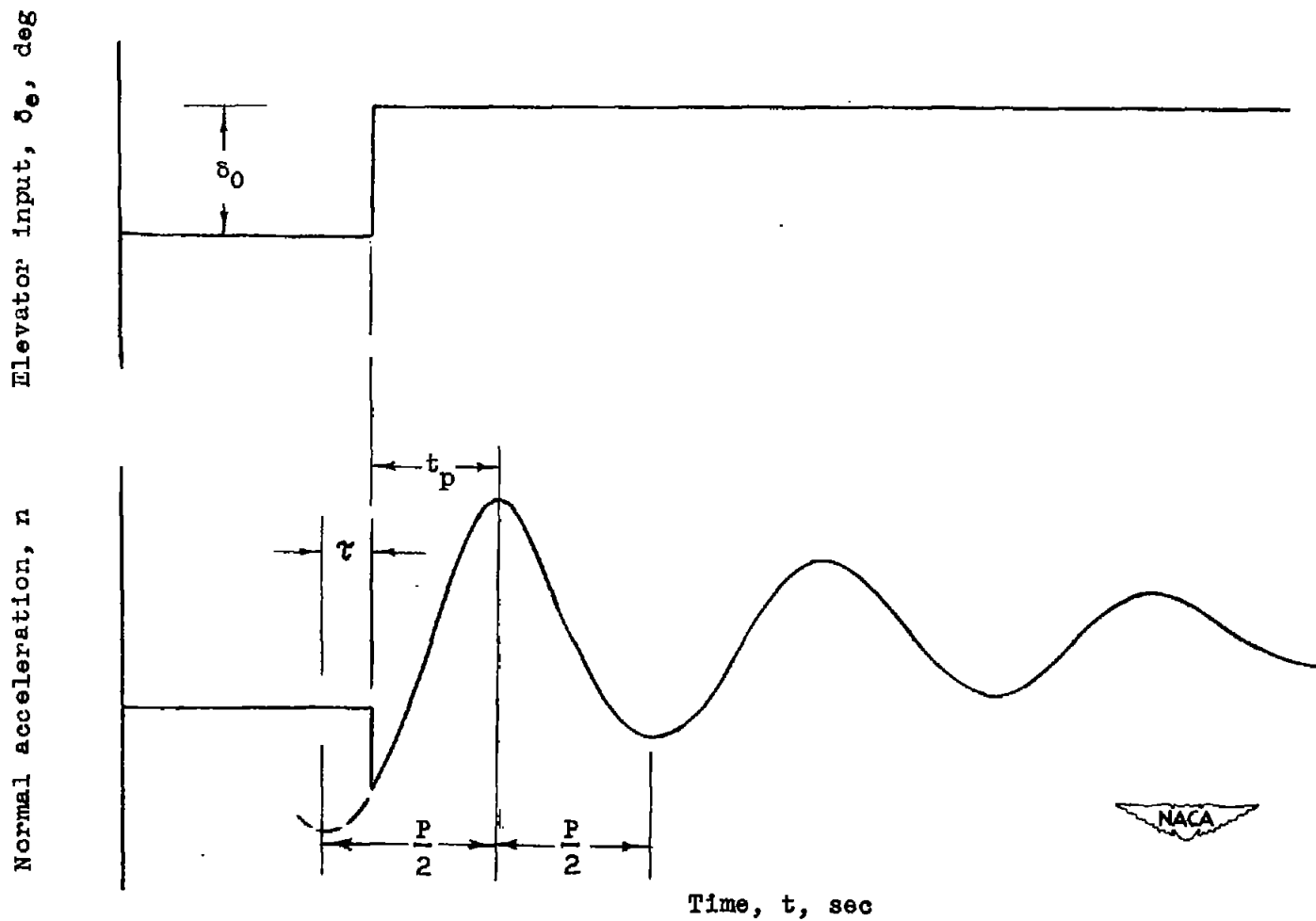


Figure 4.- Relationship of lag τ to phase angle ϕ in a time response

to a step elevator input. $\phi = 2\pi \frac{\tau}{P} = 2\pi \left(\frac{1}{2} - \frac{t_p}{P} \right)$.

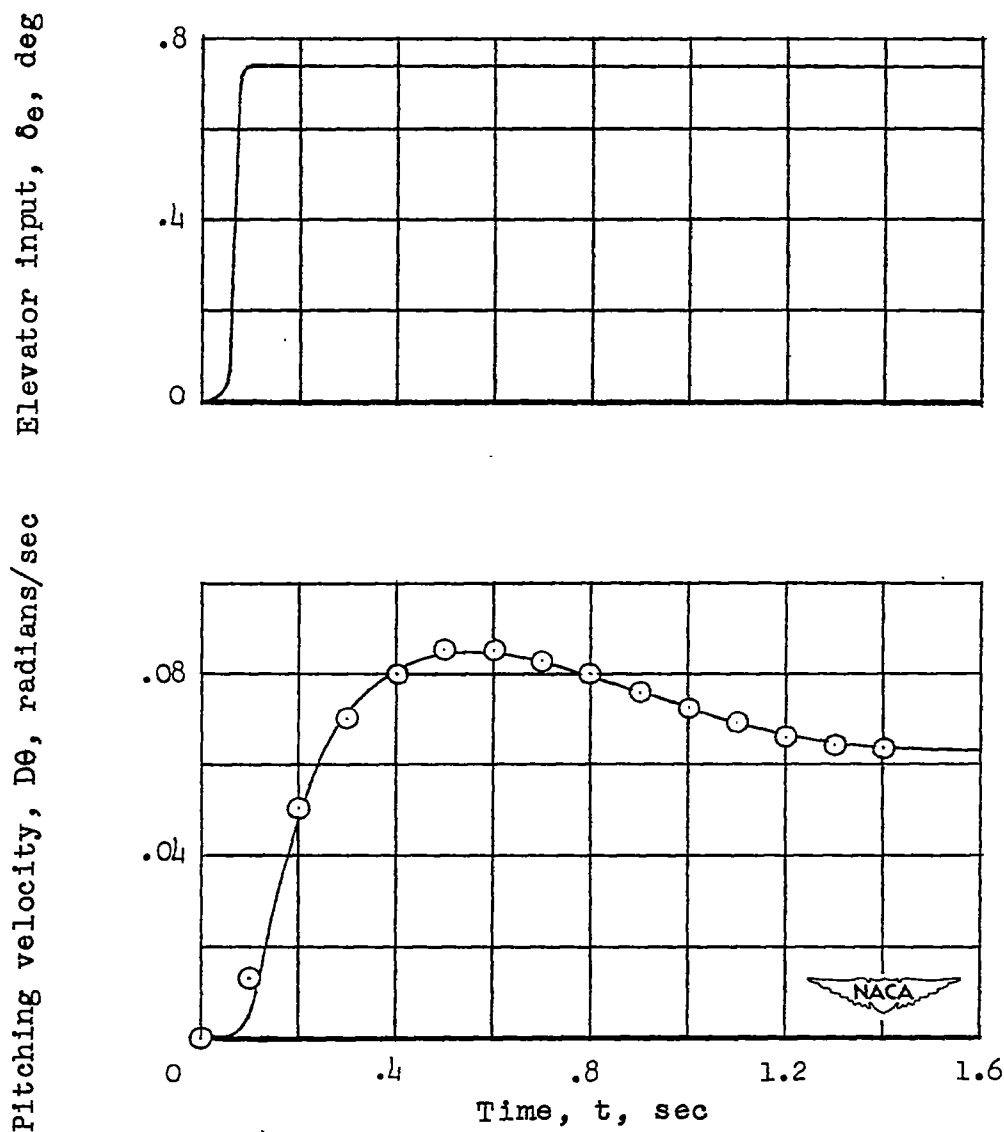


Figure 5.- Time history of elevator step input and pitching-velocity response of fighter at $M = 0.6$ and $h_p = 10,000$ feet. Circled points indicate the response calculated from transfer coefficients obtained from Donegan-Pearson method.

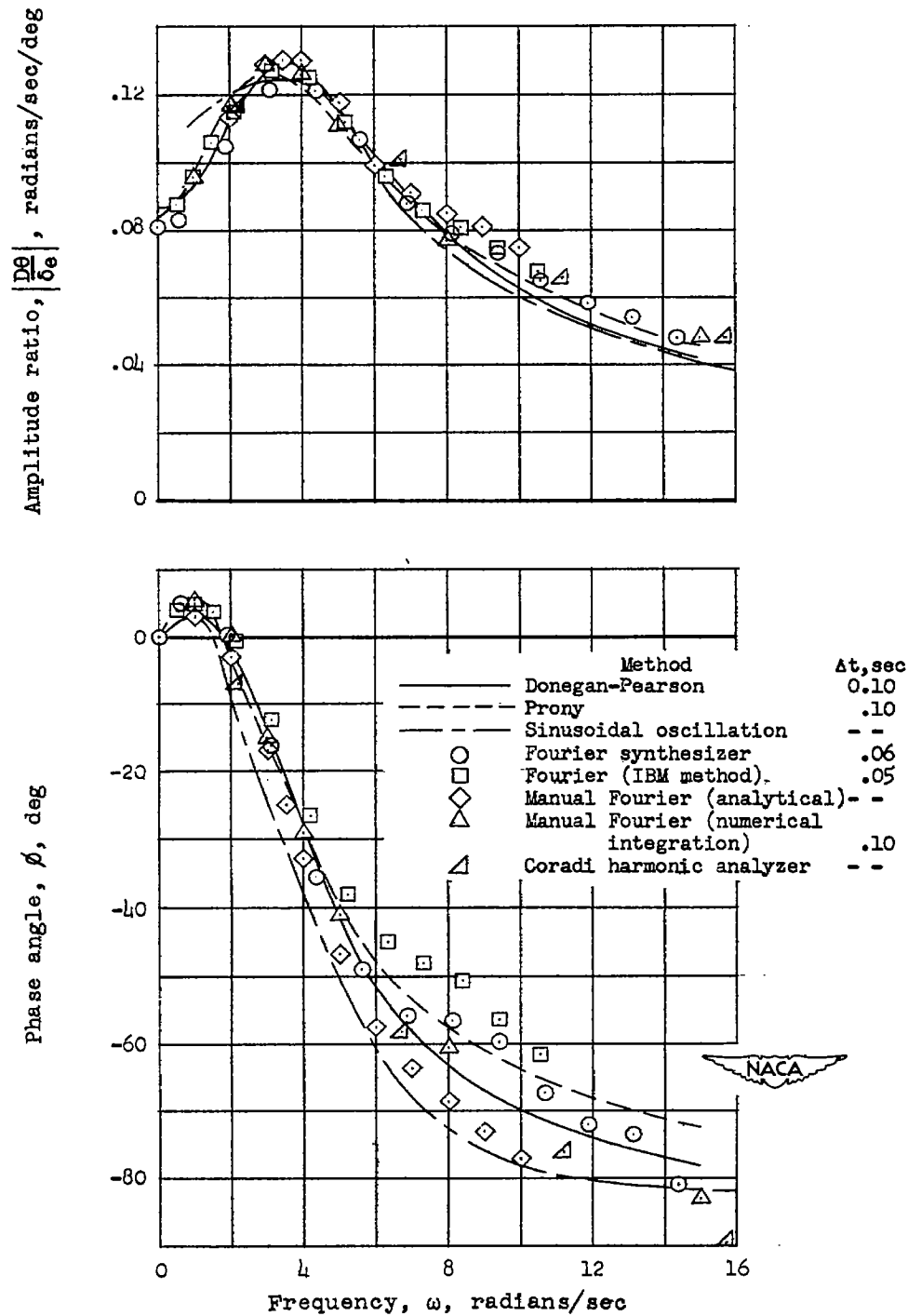


Figure 6.- Frequency response of the fighter relating pitching velocity to elevator deflection at $M = 0.6$ and $h_p = 10,000$ feet as determined by several methods.

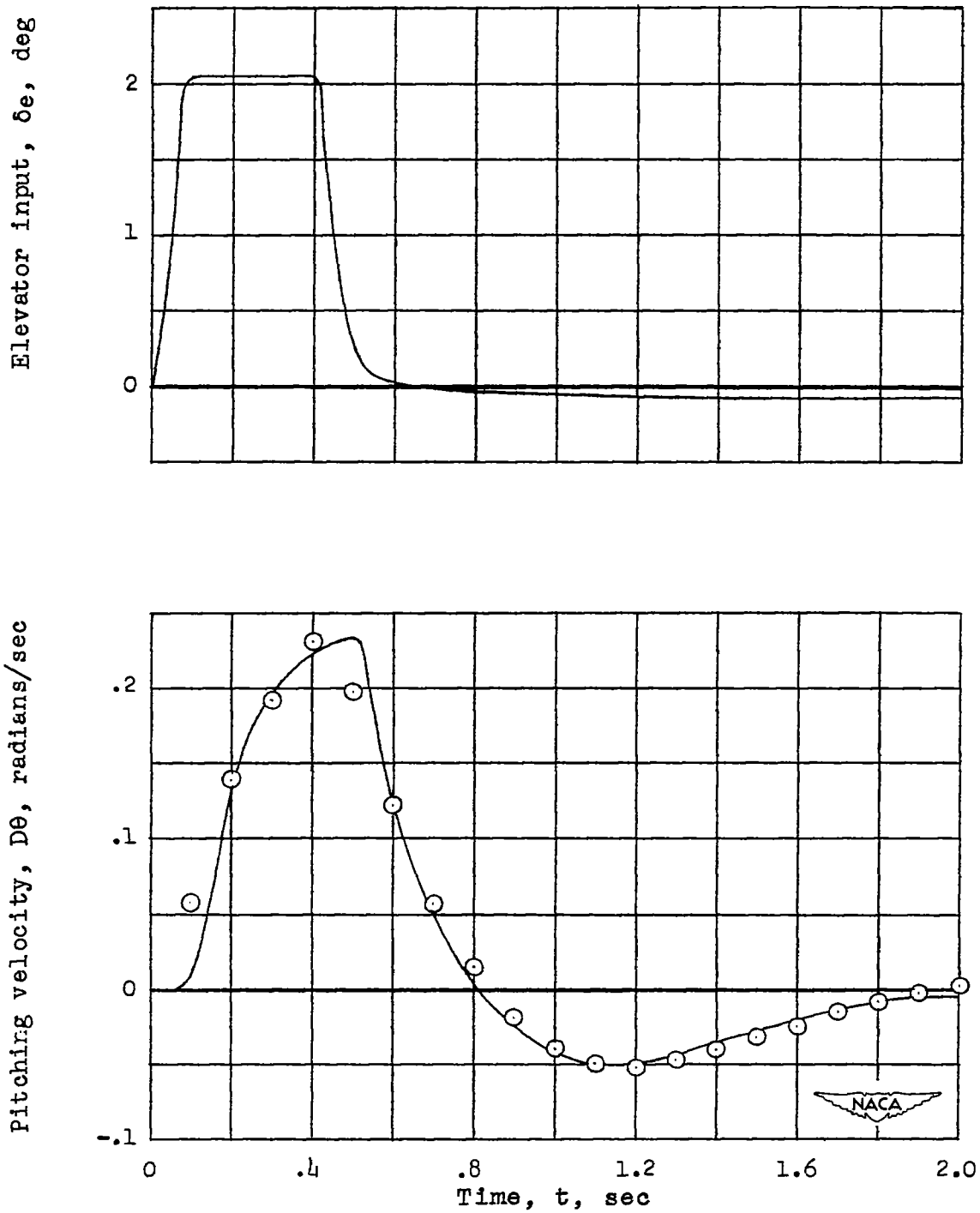


Figure 7.- Time history of elevator square-pulse input and pitching-velocity response of fighter at $M = 0.6$ and $h_p = 10,000$ feet. Circled points indicate the response calculated from transfer coefficients obtained from Donegan-Pearson method.

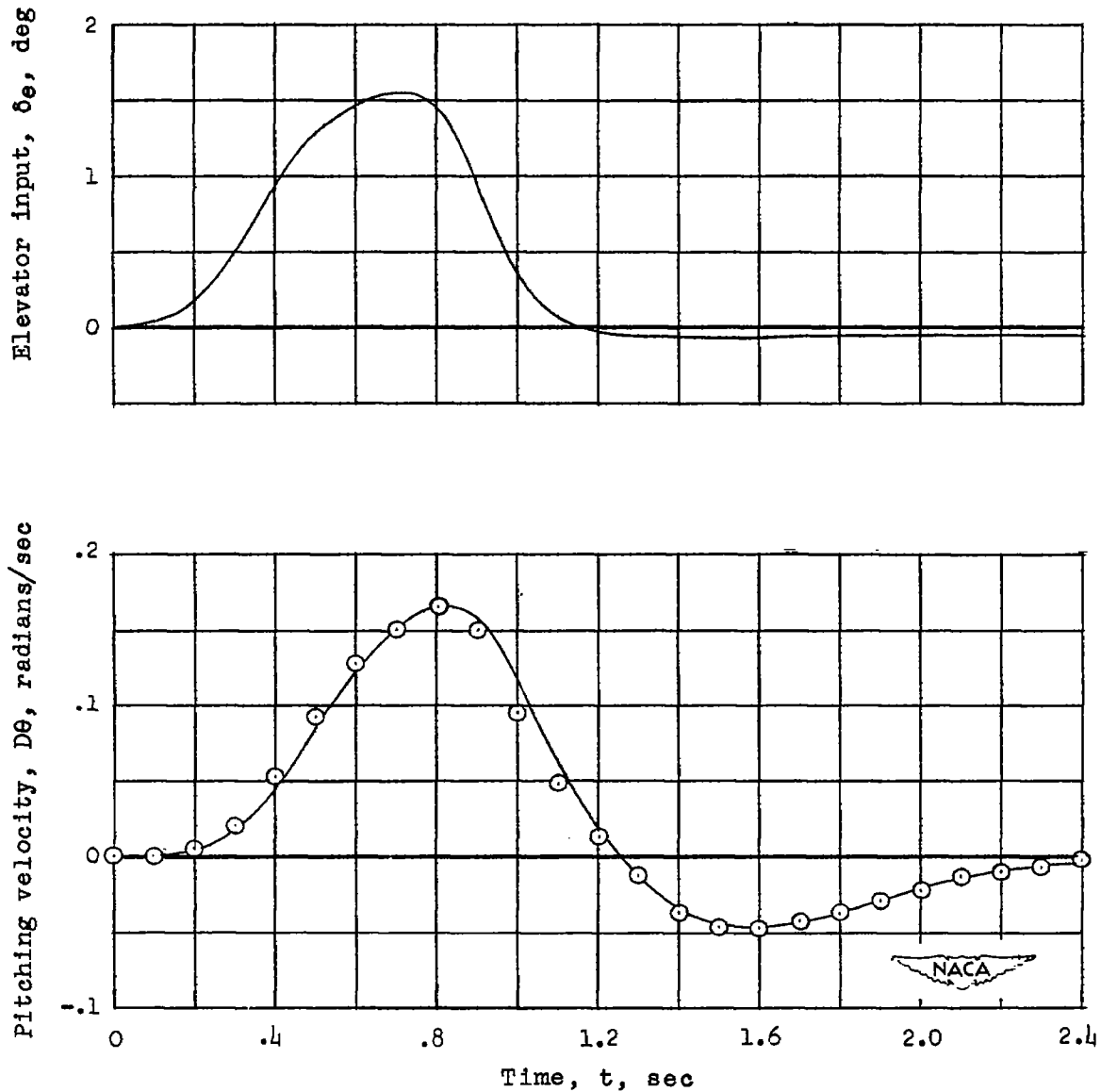


Figure 8.- Time history of elevator triangular-pulse input and pitching-velocity response of fighter at $M = 0.6$ and $h_p = 10,000$ feet. Circled points indicate the response calculated from transfer coefficients obtained from Donegan-Pearson method.

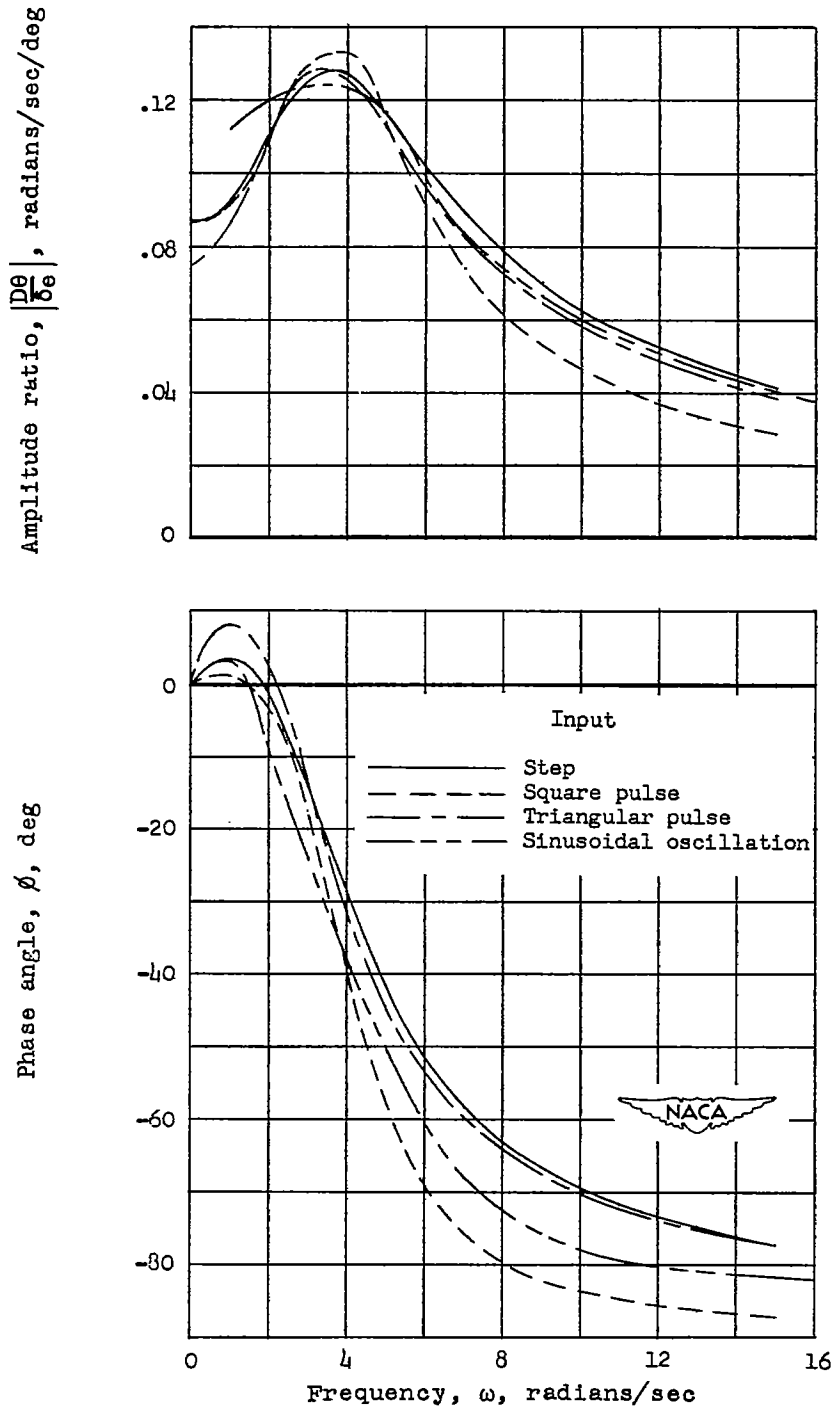


Figure 9.- Comparison of frequency-response curves of the fighter at $M = 0.6$ and $h_p = 10,000$ feet as obtained from a variety of inputs by using the Donegan-Pearson and sinusoidal-oscillation methods.

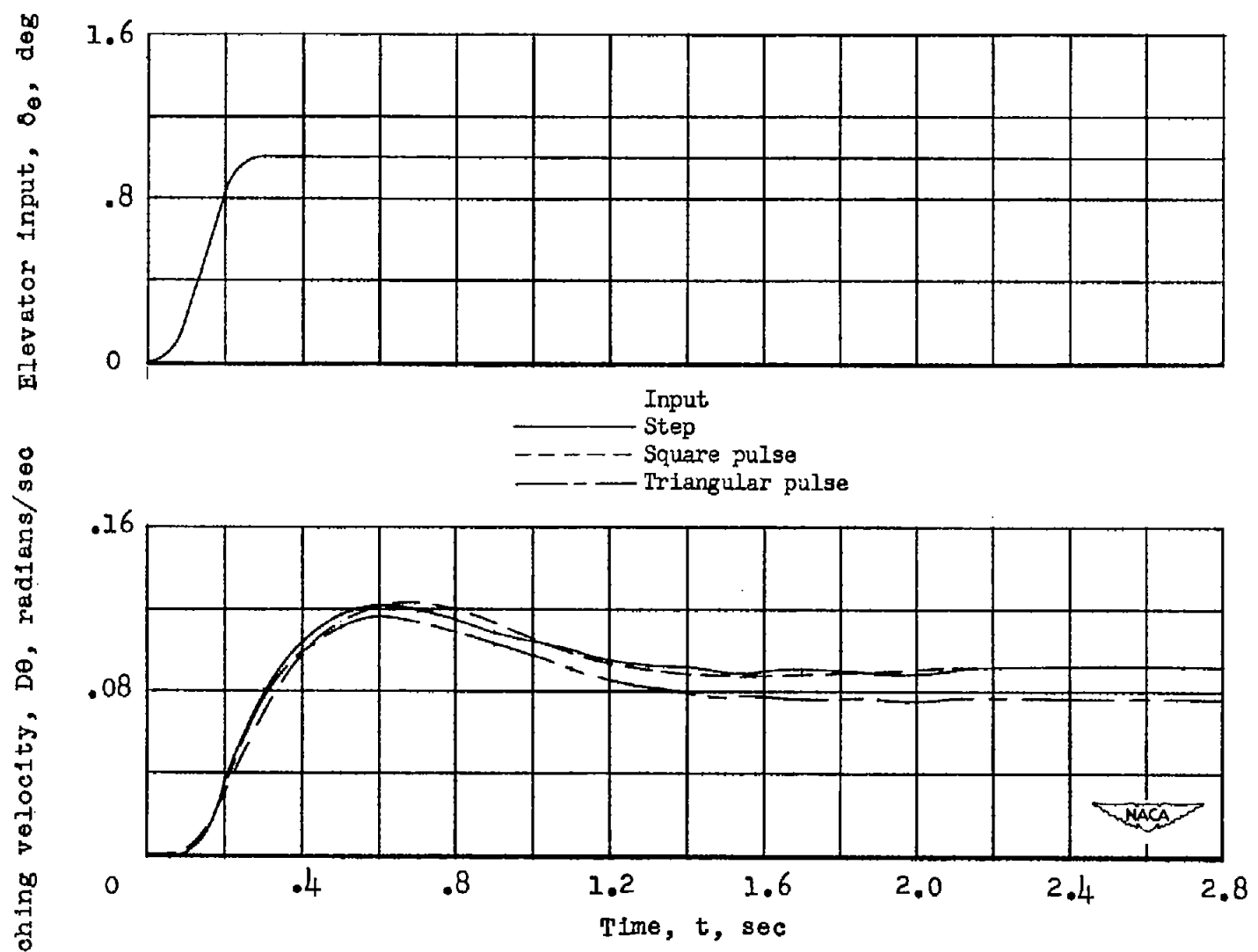


Figure 10.- Simulated elevator input and time response of fighter in pitching velocity as defined by several frequency-response curves.

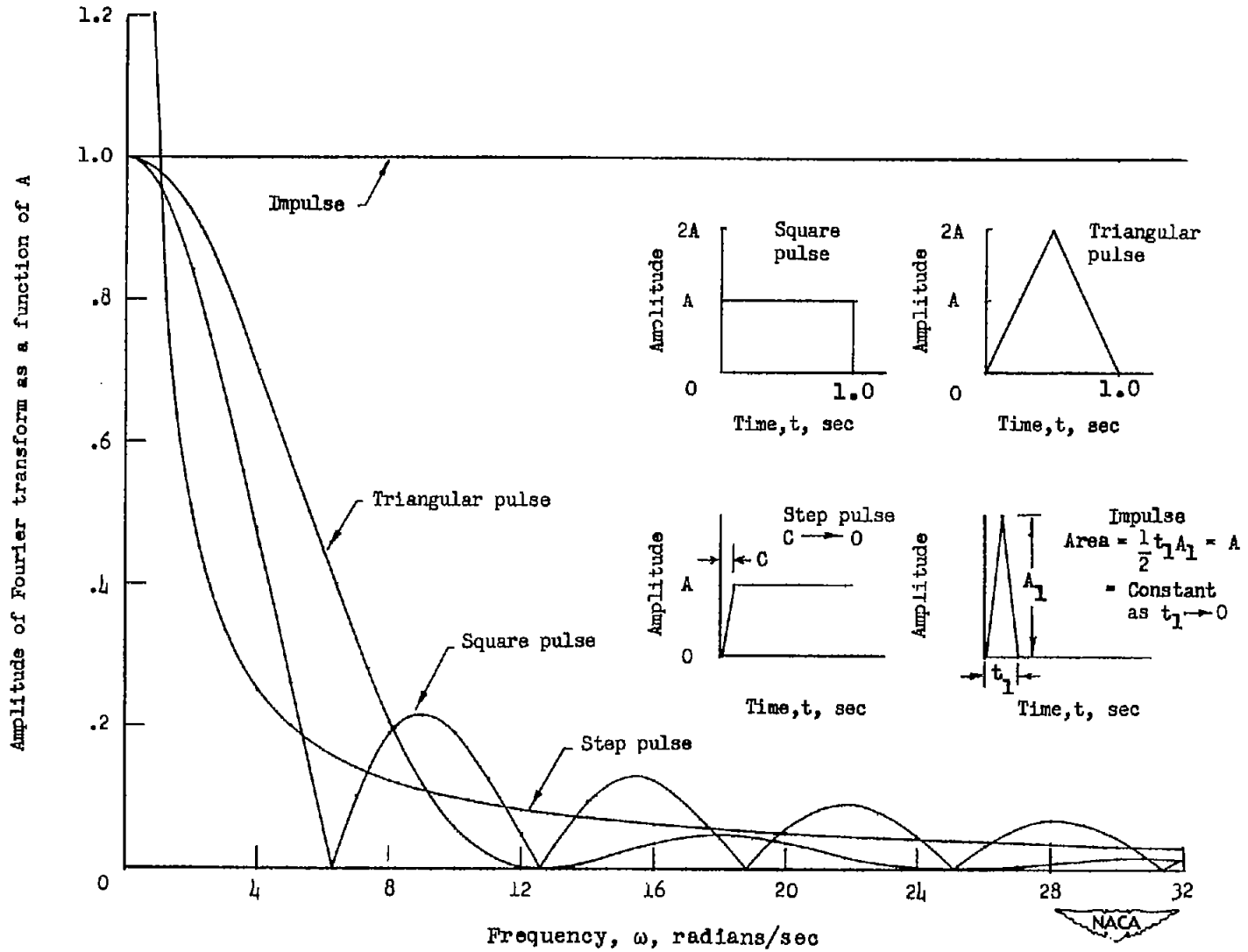


Figure 11.- Fourier transforms of several basic input shapes.

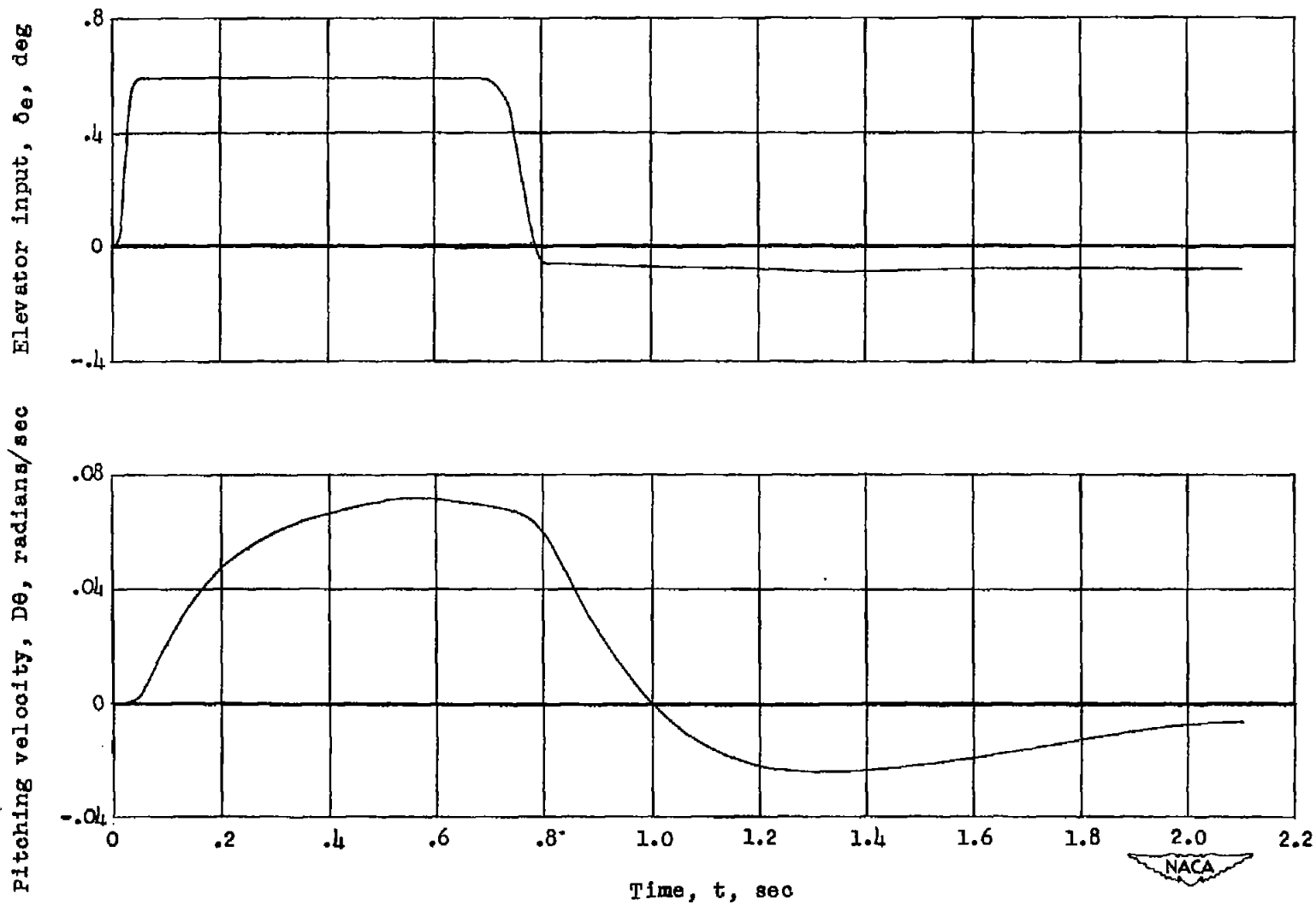


Figure 12.- Time history of elevator rectangular-pulse input and pitching-velocity response of fighter at $M = 0.6$ and $h_p = 10,000$ feet.

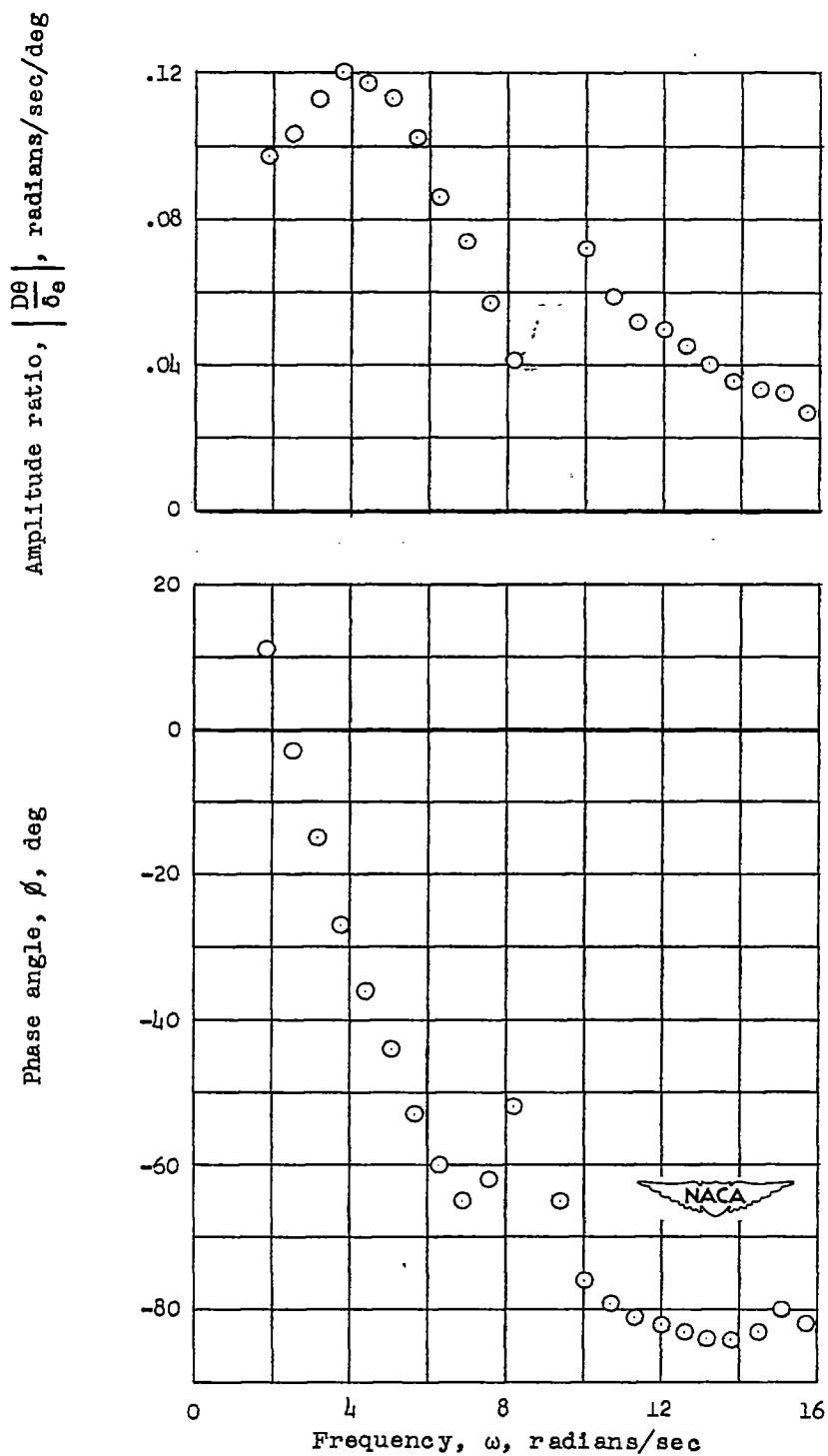


Figure 13.- Discrepancies in regions of low harmonic content that appear when the frequency response of the fighter is determined by the Fourier analysis.

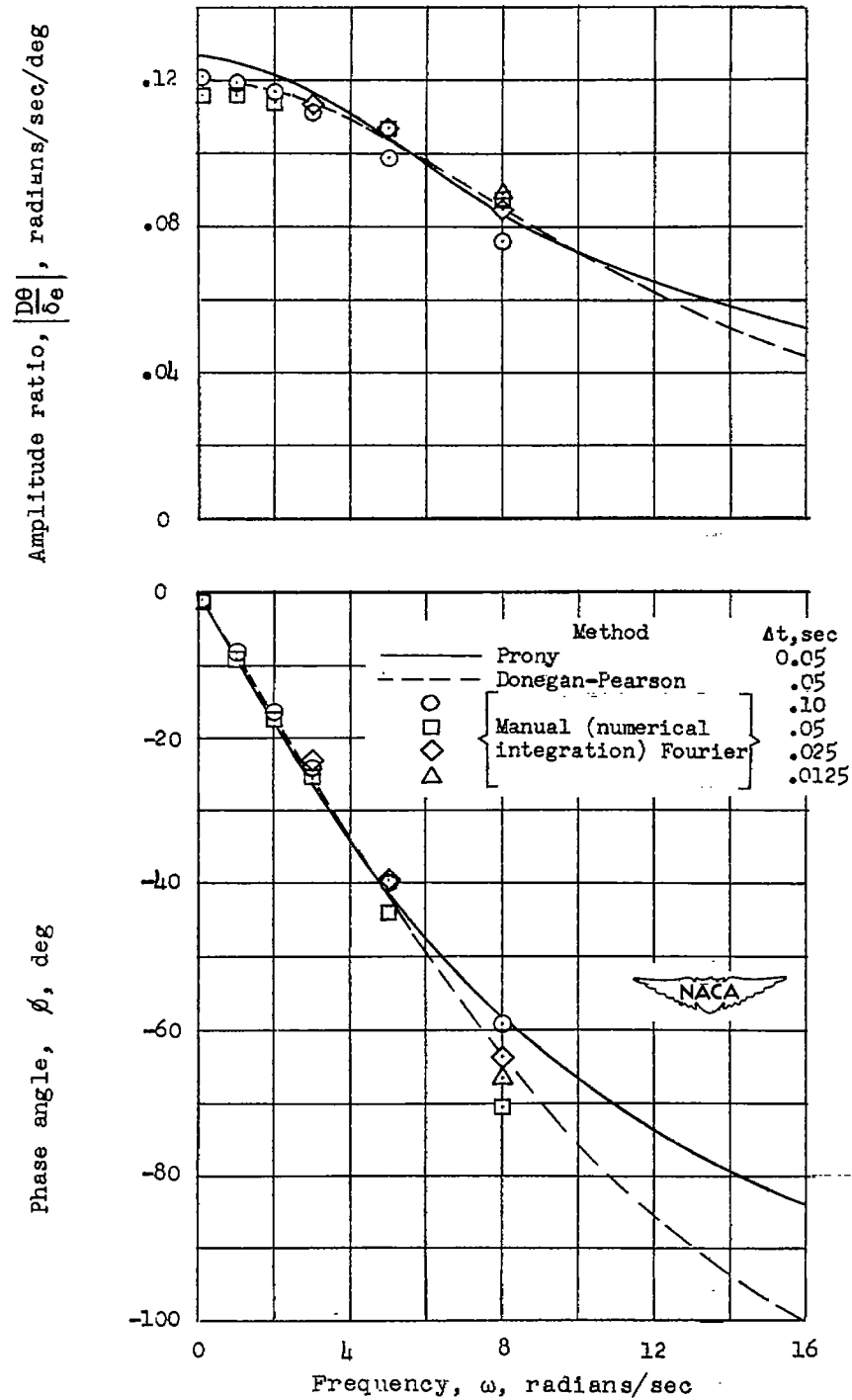


Figure 14.- Frequency response of the fighter relating pitching velocity to elevator deflection at $M = 0.6$ and $h_p = 10,000$ feet as determined from first one-third of rectangular-pulse-input time history.

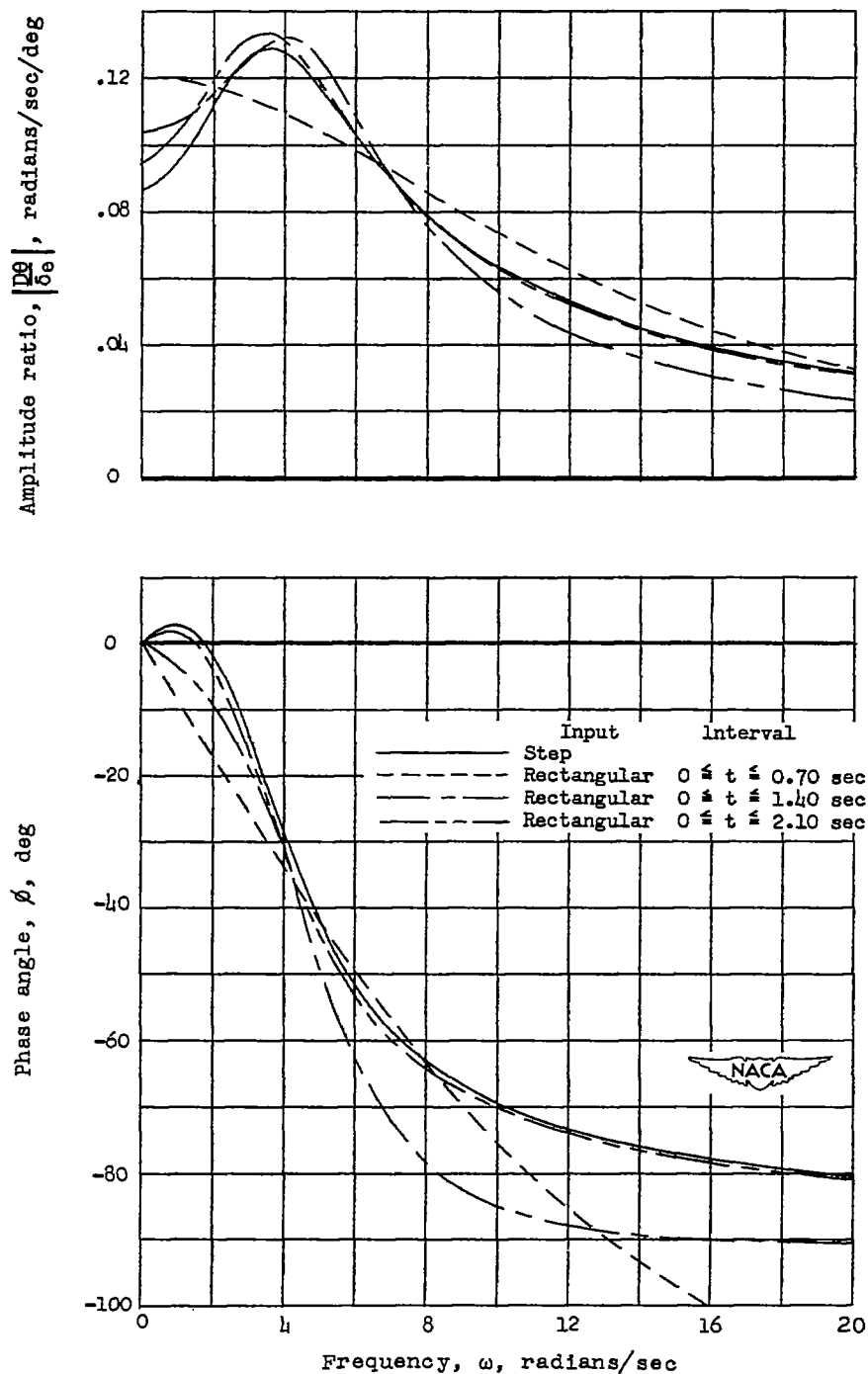
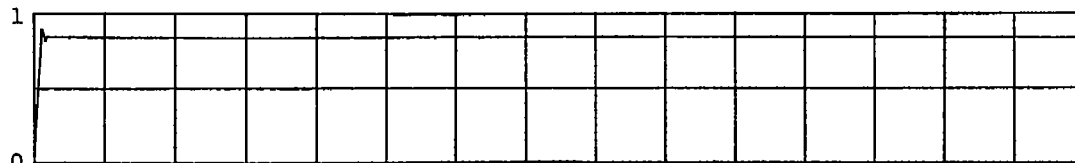


Figure 15.- Frequency response of the fighter relating pitching velocity to elevator deflection at $M = 0.6$ and $h_p = 10,000$ feet as determined from portions of rectangular-pulse- and step-input time histories by using the Donegan-Pearson method.

Elevator input, δ_e , deg



Angle of attack, α , deg

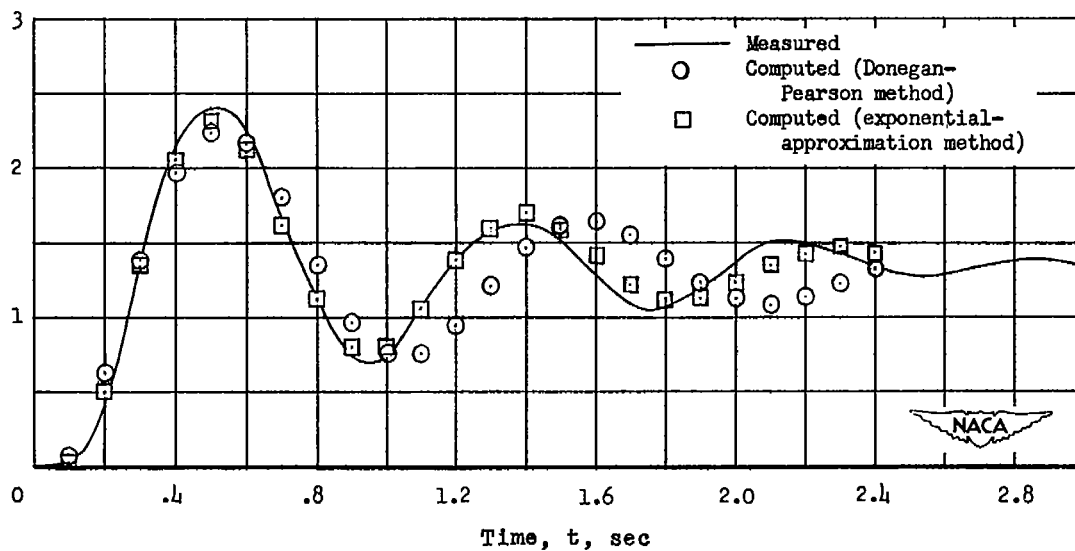


Figure 16.- Time history of elevator step input and angle-of-attack response of the free-fall model at $M = 0.725$ and $h_p = 32,000$ feet. The responses, as computed by the Donegan-Pearson and exponential-approximation methods, are indicated.

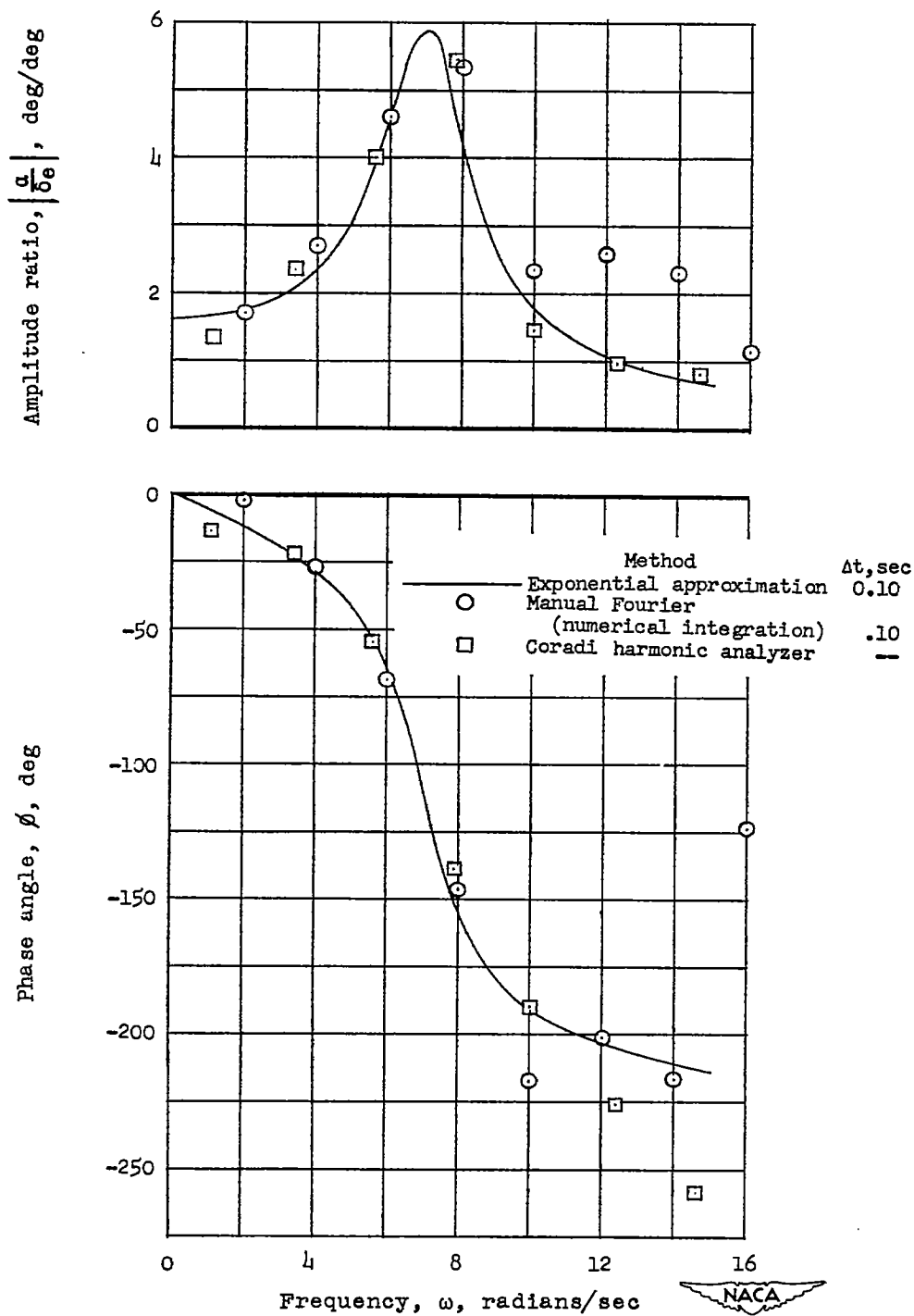


Figure 17.- Frequency response relating angle of attack to elevator deflection of a free-fall model at $M = 0.725$ and $h_p = 32,000$ feet as determined by several methods.

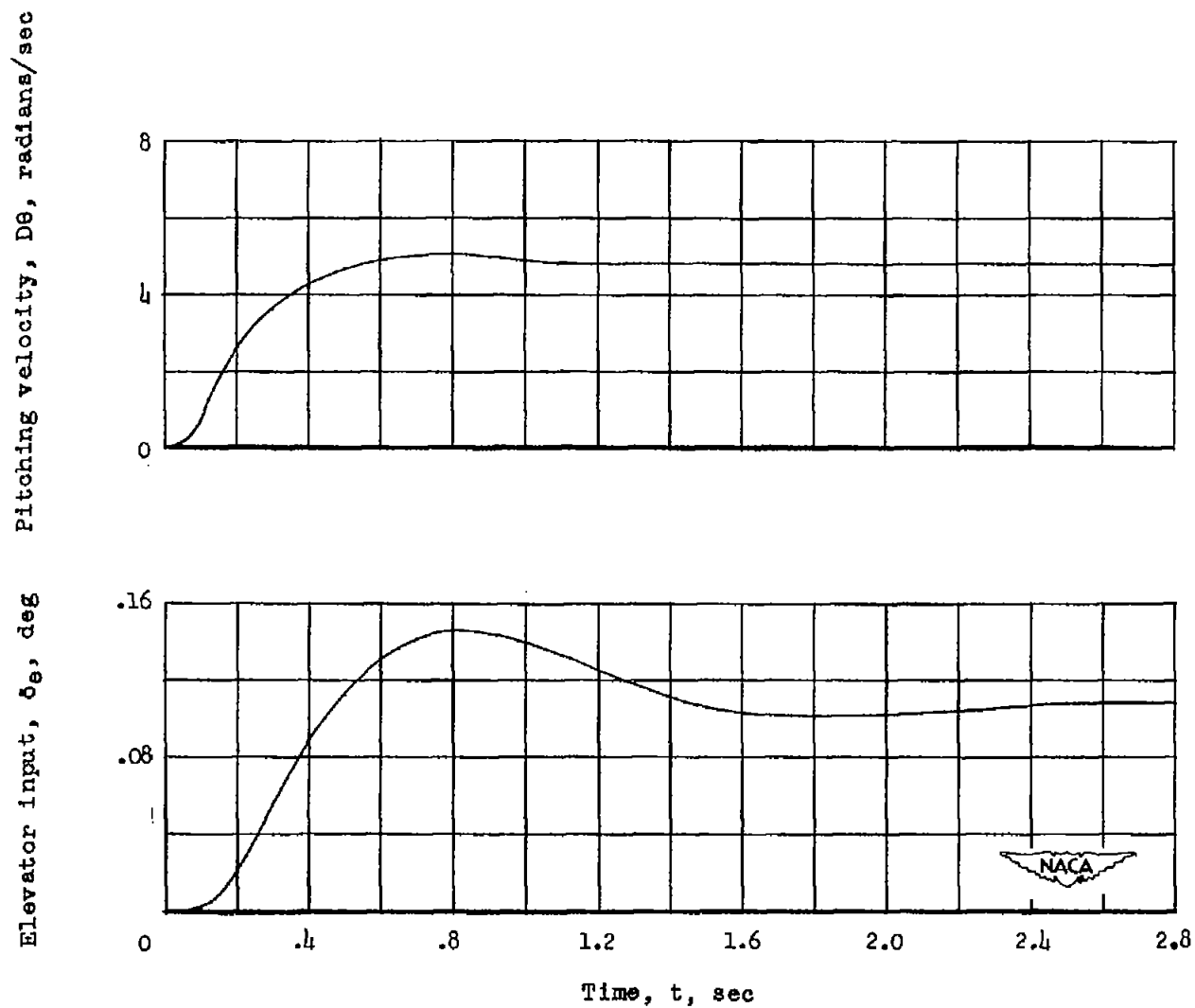


Figure 18.- Time history of elevator input and pitching-velocity response of the transport at $M = 0.268$ and $h_p = 5,000$ feet.

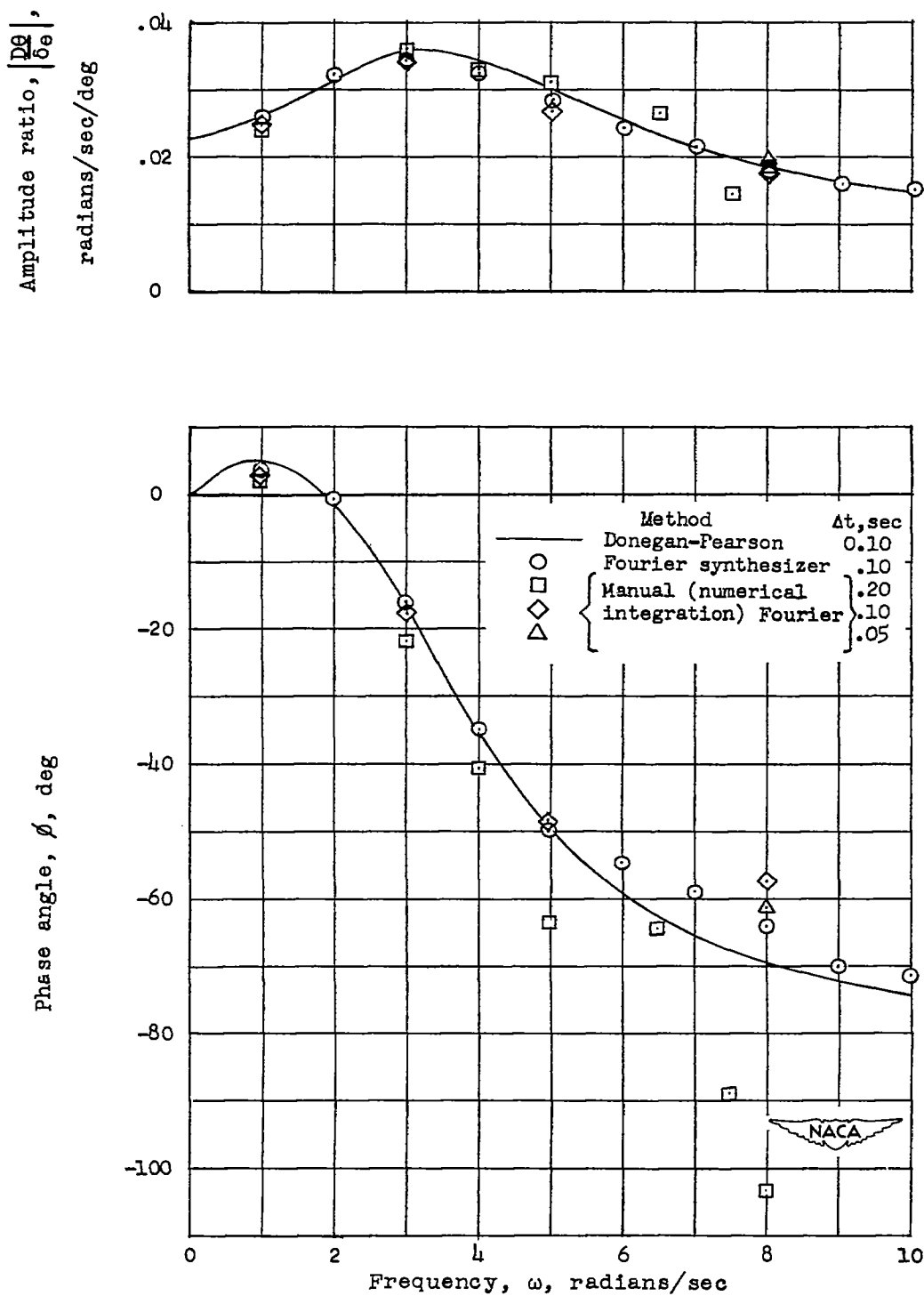


Figure 19.- Frequency response of the transport at $M = 0.268$ and $h_p = 5,000$ feet as determined by several methods.

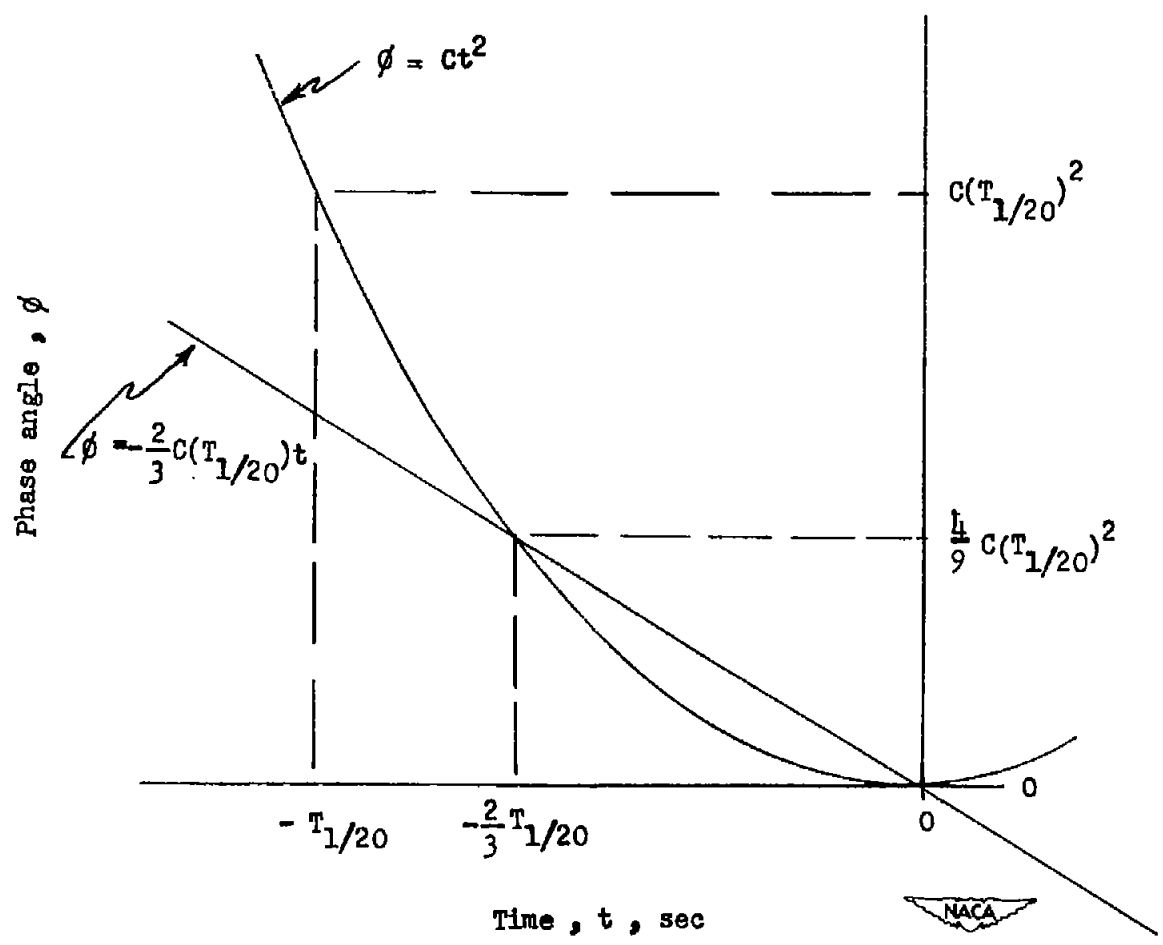


Figure 20.- Straight-line approximation to the parabolic-phase-angle variation which exists between a constant-frequency wave and a wave whose frequency changes at a constant rate.

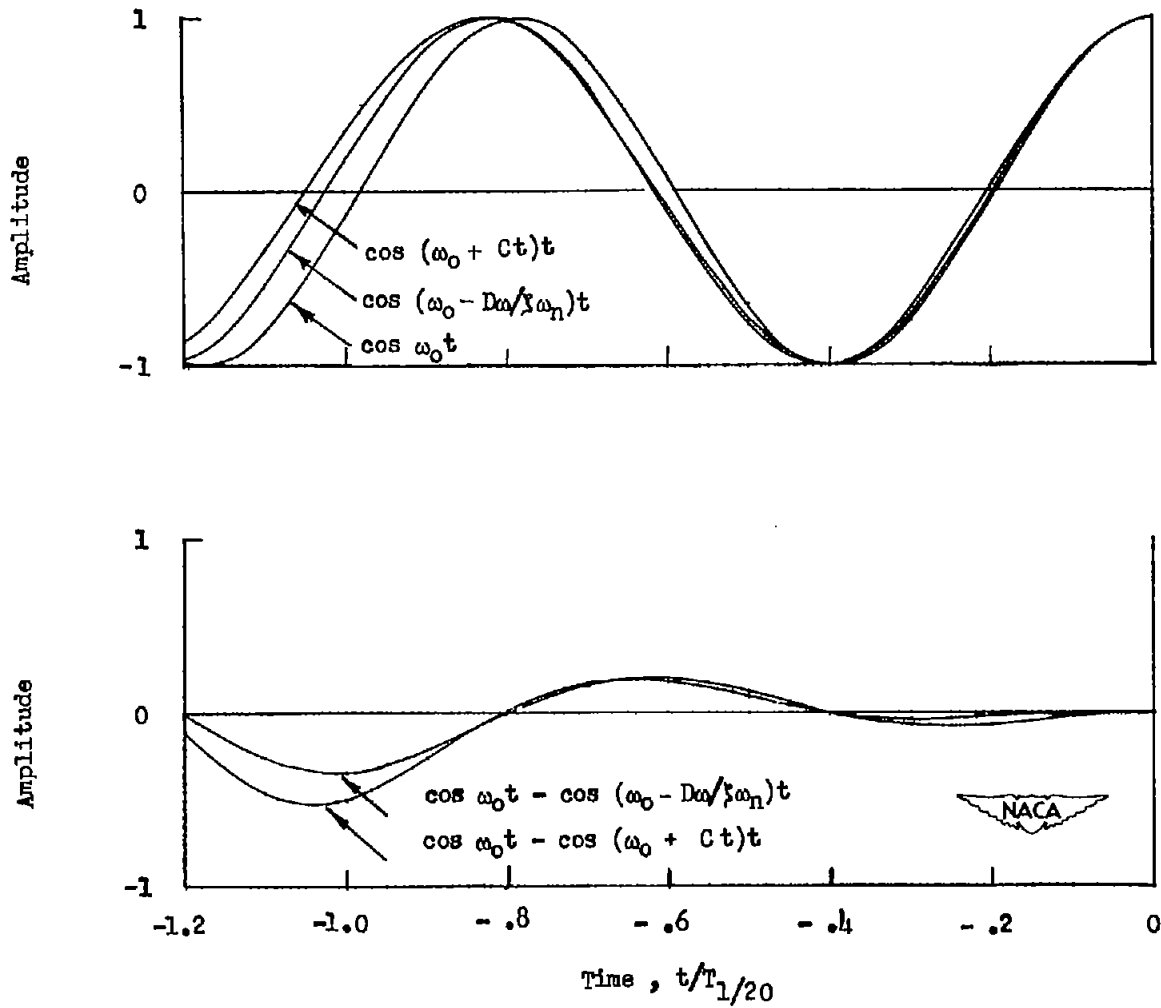


Figure 21.- Time history of cosine wave forms in the vicinity of zero time for a case where $D\omega = 1$ radian per second per second and $\omega_0 = 8$ radians per second.

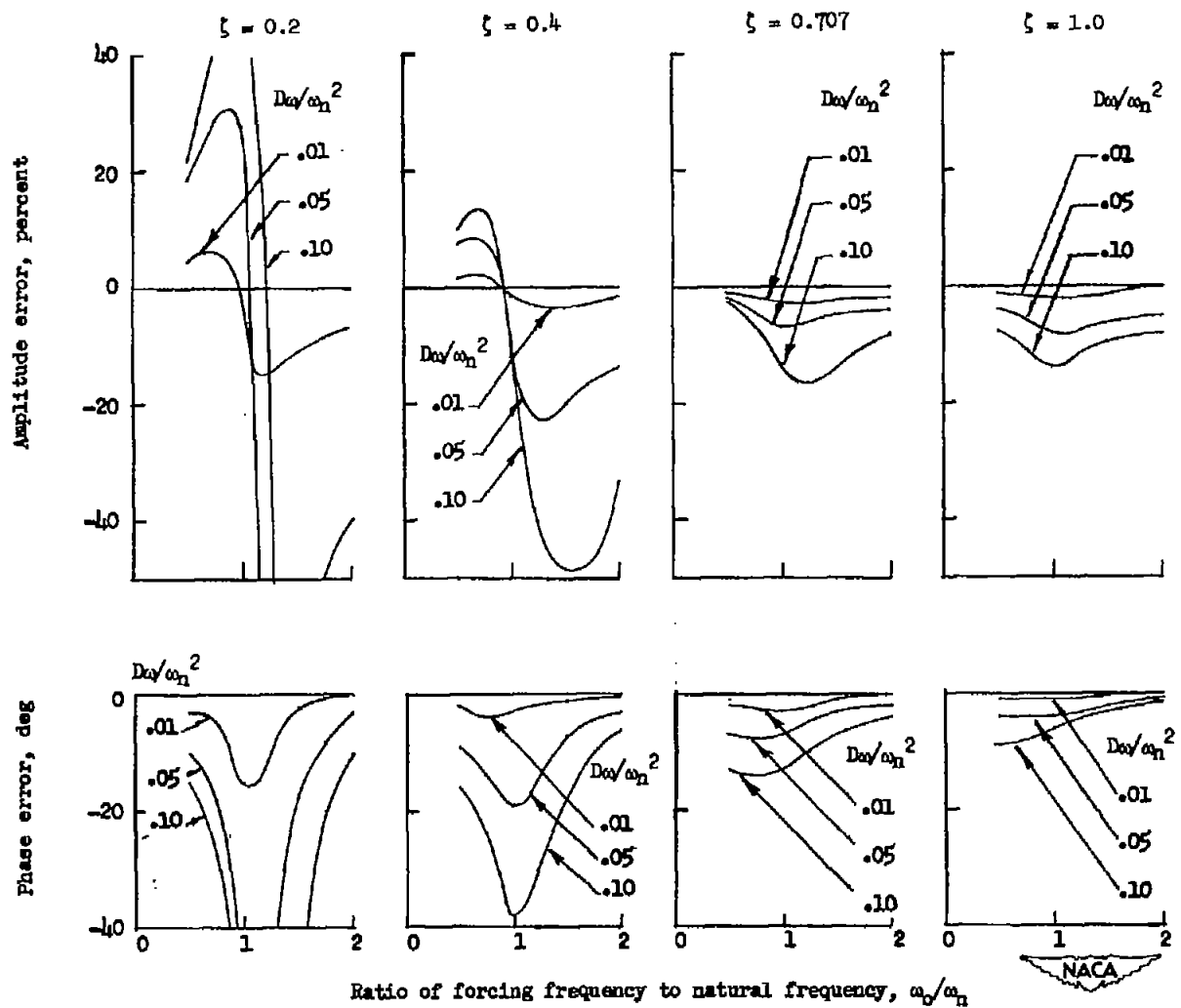


Figure 22.- Variation in amplitude and phase errors obtained when using a sinusoidal input, which changes frequency at a constant rate, to simulate a steady sinusoidal input.